

A covariant variational approach to Yang-Mills Theory at finite temperatures

M. Quandt* and H. Reinhardt†

Universität Tübingen

Institut für Theoretische Physik

Auf der Morgenstelle 14

D-72076 Tübingen, Germany

(Dated: July 31, 2021)

Abstract

We extend the covariant variational approach for $SU(N)$ Yang-Mills theory in Landau gauge to non-zero temperatures. The renormalization of the zero-temperature case is revisited and it is shown that the same counterterms are sufficient to render the low-order Green's function finite at non-zero temperature. We compute the ghost and gluon propagator numerically and show that it agrees in all qualitative respects with the results of high-precision lattice calculations.

PACS numbers: 11.80.Fv, 11.15.-q

Keywords: gauge theories, confinement, variational methods, Landau gauge

* markus.quandt@uni-tuebingen.de

† hugo.reinhardt@uni-tuebingen.de

I. INTRODUCTION

In recent years functional continuum methods have been extensively used to study the low energy sector and the phase diagram of quantum chromodynamics (QCD). These methods include functional renormalization group (FRG) flow equations [1–3], Dyson-Schwinger equations (DSE) [4, 5] and variational methods [6–8]. The gauge-variance of the Green’s functions makes it necessary to fix a gauge, and most techniques such as FRG and DSE initially concentrated their studies on the case of covariant gauges. This choice has a two-fold advantage: On the one hand, the BRST symmetry and the ensuing Slavnov-Taylor identities provide constraints to guide the analysis. More importantly, however, the Kugo-Ojima criterion [9, 10] claims a direct connection, based on the BRST mechanism, between the propagators in Landau gauge and physical phenomena such as colour confinement.

At the quantum level, it is not immediately clear if BRST symmetry is naively maintained or visible. Most of the functional studies quoted above initially found an infrared vanishing, *scaling* type of solution for the gluon propagator (as the Kugo-Ojima criterion would suggest), which is, however, at odds with high-precision lattice simulations [11–14]. It was later shown that infrared finite *decoupling* solutions could also be obtained, if the infrared behaviour is sufficiently constrained [15]; such solutions had also been found earlier [16–32]. The decoupling solutions agree very well with lattice data, but indicate a (soft) BRST breaking in the full theory.

In Ref. [6], we proposed a variational approach that is based on the effective action for the gluon propagator. The technique offers several conceptual advantages: For instance, it automatically yields a closed set of integral equations that can be renormalized through conventional counter terms without further truncation. In addition, the variational approach allows, in principle, to discern between the scaling and decoupling type of solution, as the one with the lower effective action must be realized. Numerically, the approach yields excellent agreement with lattice data that is on par with the best functional methods listed above.

On the other hand, the variational approach violates BRST symmetry and the Kugo-Ojima criterion does not apply so that the question of colour confinement in the variational approach is mute at the moment. This explicit violation of BRST symmetry is unavoidable (to a certain extent) in *any* analytical approach, and it is important that the breaking occurs in a controlled way. For the variational approach, BRST symmetry is implemented exactly in the target func-

tional and an unconstrained variation will give the exact solution. It is only through restrictions on the trial variation measure that the breaking of BRST symmetry occurs. As we enlarge the variational ansatz space, we improve the quality of the dynamics, and at the same time reduce the violation of BRST symmetry (even though we do not have a reliable measure to quantify this).¹ The situation is, in fact, analogous to the Hamiltonian formulation in Coulomb gauge [7, 33–36] where Gauss’ law can be implemented exactly in the target Hamiltonian, but only the exact solution of the functional Schrödinger equation will obey Gauss’ law exactly. Numerically, the variational solution of Ref. [6] describes the propagators very well, particularly in the mid-momentum region which is most important phenomenologically, especially for the deconfinement phase transition. It is therefore natural to extend this approach to finite temperatures and finite chemical potentials, and eventually include dynamical fermions. In the present paper, we describe the first step in this program, viz. the introduction of non-zero temperature. Naturally, this extension has also been done in the FRG [37] and DSE [38] as well as in a perturbative approach [39, 40]. The lattice data [41] show a cross-over type of signal in the ratio of the two inequivalent Lorentz structures for the gluon propagator, but no clear qualitative change at the deconfinement phase transition. In the present paper, we will concentrate on the finite-temperature propagators and search for signals of a phase transition that can be derived from them alone. Eventually, the present work should be extended to measure the effective action for the Polyakov loop, which is the real order parameter for Yang-Mills theory at finite temperature. This study will be reported elsewhere.

The paper is organised as follows: In the next section, we revisit the covariant variational principle and extend it to finite temperatures through the imaginary time formalism. In section III we compute the effective action for the gluon propagator at finite temperature and derive the unrenormalized gap equation. Section IV simplifies and improves the renormalization at zero temperature discussed in Ref. [6]. We demonstrate that the same counter terms are also sufficient to render the theory finite at any non-zero temperature, and present the fully renormalized finite-temperature corrections to the integral equations. In section V, we report our numerical treatment and present solutions for the ghost and gluon propagator. In particular, we study possible signals for a phase transition in the gluon and ghost propagator. In the last section, we conclude this study with a brief summary and an outlook on further extensions of

¹ This is consistent since symmetries are invariances of the dynamics, i.e. it is not necessary nor appropriate to enforce a symmetry of the exact model onto the truncated dynamics.

the variational method.

II. THE VARIATIONAL PRINCIPLE

A. The variational method at finite temperatures

In Ref. [6], we described the basics of the covariant variational principle in quantum field theory: for a theory with a quantum field A defined by an action $S(A)$ in Euclidean space time, the variation is over all normalised path integral (probability) measures $d\mu(A)$ used to compute quantum averages according to $\langle \cdots \rangle_\mu \equiv \int d\mu(A) \cdots$. If the measure is written in Radon-Nikodym form $d\mu(A) = dA \rho(A)$ with a suitable density ρ , the *entropy*

$$\mathcal{W}(\mu) \equiv -\langle \ln \rho \rangle_\mu = - \int dA \rho(A) \ln \rho(A) \quad (1)$$

describes the accessible field space for quantum fluctuations. In the full theory, the entropy of the fluctuations is balanced against the classical Euclidean action such that the *free action*

$$F(\mu) \equiv \langle S \rangle_\mu - \hbar \mathcal{W}(\mu) \stackrel{!}{=} \min \quad (2)$$

is minimized. This is because the unique solution of the variational principle (2) is the Gibbs-like measure

$$d\mu_0(A) = Z^{-1} \exp \left[-\hbar^{-1} S(A) \right] dA \quad (3)$$

whose moments are the conventional Schwinger functions; the minimal free action is simply $F(\mu_0) = -\ln Z$. The *quantum effective action* is a constrained version of the free action,

$$\Gamma(\omega) \equiv \min_\mu F(\mu, \omega) \equiv \min_\mu \left\{ \langle S \rangle_\mu - \hbar \mathcal{W}(\mu) \mid \langle \Omega \rangle_\mu = \omega \right\}, \quad (4)$$

where an arbitrary operator Ω is fixed to a prescribed external value ω . Usually, Ω is chosen as the quantum field operator A itself whence ω becomes the *classical field*, but this is not mandatory: for the present study, it is more convenient to take Ω as the 2-point function of the quantum field and compute the optimal propagator from the overall minimisation of the effective action, $\delta\Gamma/\delta\omega = 0$.

To transcribe this method to non-zero temperatures, we can follow the standard imaginary time formalism and restrict the Euclidean time interval to $[0, \beta]$ with anti/periodic temporal

boundary conditions for fermions/bosons, respectively. This procedure works because the free action in our approach is always computed from a conventional quantum field theory, in which temperature can be introduced as described. The minimal free action eq. (2) obtained for the Gibbs measure is still $F(\mu_0) = -\ln Z$, but with the partition function

$$Z(\beta) = \int_{\beta} dA \exp \left[-\hbar^{-1} S(A) \right] \quad (5)$$

now computed using fields with the appropriate temporal boundary conditions. With the corresponding Fourier decomposition (in the bosonic case)

$$A(t, \mathbf{x}) = \beta^{-1} \sum_{n \in \mathbb{Z}} \int \frac{d^3 k}{(2\pi)^3} e^{i(v_n t + \mathbf{k} \cdot \mathbf{x})} A_n(\mathbf{k}), \quad v_n = \frac{2\pi}{\beta} n \quad (n \in \mathbb{Z}) \quad (6)$$

and translational invariance (in both space and time separately), it is easy to see that the space-time volume factorizes, $F(\mu_0) = -\ln Z(\beta) = \beta V \cdot f$. The free action density f obtained in this way agrees, in the free case, with the thermodynamical free energy density of a non-interacting grand-canonical Bose gas (including the self-energy), provided that the path integral measure was properly normalized² [42]. This observation generalizes to interacting field theories, and in particular to gauge theories. In the latter case, the inclusion of the Faddeev-Popov (FP) determinant is crucial, and the Matsubara frequencies for the FP ghost fields must involve *even* multiples of π/β (as in eq. (6)) even though the ghost fields obey Fermi statistics [42].

The inclusion of the ghost fields also requires an adaption of the variational principle: since the FP determinant $\mathcal{J}(A)$ describes the natural measure on the orbit space of the gauge fixed theory, the entropy of all trial measures must be computed *relative* to the FP determinant, which amounts to replacing the entropy by the relative entropy [6]

$$\overline{\mathcal{W}}(\mu) \equiv \mathcal{W}(\mu) + \langle \ln(\mathcal{J}) \rangle_{\mu} = -\langle \ln(\rho/\mathcal{J}) \rangle_{\mu}. \quad (7)$$

B. Gaussian trial measures

The zero-temperature investigations in Ref. [6] have shown that a Gaussian ansatz for the path integral measure $d\mu$ is sufficient to describe the propagators of the theory accurately. We will therefore try a similar ansatz at finite temperatures,

$$d\mu(A) = \mathcal{N} \cdot dA \mathcal{J}(A)^{1-2\alpha} \cdot \exp \left[-\frac{1}{2} \int_{\beta} d^4(x, y) A_{\mu}^a(x) \delta^{ab} \omega_{\mu\nu}(x, y) A_{\nu}(y) \right], \quad (8)$$

² This equality holds in units where $\hbar = 1$ and the Boltzmann constant $k_B = 1$, which we assume from here on.

where α is a variational parameter and the normalisation \mathcal{N} depends, in general, on α and on the kernel ω . We have also assumed that the kernel ω can be taken colour diagonal because of global colour invariance left after (covariant) gauge fixing. Finally, we have also introduced the abbreviation

$$\int_{\beta} dx \cdots \equiv \int_0^{\beta} dt \int_V d^3x \cdots \quad (9)$$

for the spacetime integral at finite temperature. The corresponding momentum integral is

$$\int_{\beta} \mathbf{d}k f(k) \equiv \beta^{-1} \sum_{n \in \mathbb{Z}} \int \frac{d^3k}{(2\pi)^3} f(v_n, \mathbf{k}) \cdots, \quad (10)$$

i.e. the integral over k_0 is always understood as a discrete sum over the Matsubara frequencies $k_0 = v_n = 2\pi n/\beta$. The overall physical picture conveyed by the ansatz eq. (8) is a weakly interacting (constituent) gluon with an enhanced weight (for $\alpha > 0$) near the Gribov horizon.

It is clear that the gauge field must be Fourier decomposed as in eq. (6); similarly, the FP determinant for covariant gauges

$$\mathcal{J}(A) \equiv \text{Det} \left[-\partial_{\mu} \hat{D}_{\mu}^{ab} \right] / \text{Det} \left[-\square \delta^{ab} \right] = \text{Det} \left[-\square \delta^{ab} - g \partial_{\mu} f^{abc} A_{\mu}^c \right] / \text{Det} \left[-\square \delta^{ab} \right] \quad (11)$$

must be evaluated with periodic boundary conditions in time (even though the ghosts obey Fermi statistics).

Let us next look at the gluon propagator

$$\langle A_{\mu}^a(x) A_{\nu}^b(y) \rangle = \int_{\beta} \mathbf{d}k e^{ik(x-y)} \cdot \delta^{ab} D_{\mu\nu}(k). \quad (12)$$

At finite temperatures, $D_{\mu\nu}(k)$ is still a symmetric rank-2 tensor, but the overall $O(4)$ Lorentz invariance is broken because the heat bath singles out a rest frame specified by $u_{\mu} = (1, 0, 0, 0)$. Assuming that the remaining *spatial* $O(3)$ symmetry remains unbroken, $D_{\mu\nu}(k)$ must be a linear combination of all $O(3)$ -invariant symmetric rank-2 tensors that can be formed from k_{μ} and u_{μ} . Furthermore, BRST invariance entails the Ward identity for the longitudinal propagator,

$$k^{\mu} k^{\mu} D_{\mu\nu}(k) = \zeta, \quad (13)$$

where ζ is the coefficient for the gauge fixing term in covariant gauges, $\mathcal{L}_{\text{fix}} = \frac{1}{2\zeta} (\partial_\mu A_\mu^a)^2$. From all these constraints, the gluon propagator has just *two* remaining Lorentz structures,³

$$D_{\mu\nu}(k) = D_\perp(k) \mathcal{P}_{\mu\nu}^\perp(k) + D_\parallel(k) \mathcal{P}_{\mu\nu}^\parallel(k) + \frac{\zeta}{k^2} \frac{k_\mu k_\nu}{k^2} \quad (14)$$

$$D_{\mu\nu}^{-1}(k) = D_\perp^{-1}(k) \mathcal{P}_{\mu\nu}^\perp(k) + D_\parallel^{-1}(k) \mathcal{P}_{\mu\nu}^\parallel(k) + \frac{k_\mu k_\nu}{\zeta}. \quad (15)$$

The two projectors \mathcal{P}^\perp and \mathcal{P}^\parallel are both 4-dimensionally transversal, but \mathcal{P}^\perp is also 3-dimensionally transversal, while \mathcal{P}^\parallel is 3-dimensionally longitudinal,

$$\mathcal{P}_{\mu\nu}^\perp(k) = (1 - \delta_{\mu 0})(1 - \delta_{\nu 0}) \left(\delta_{\mu\nu} - \frac{k_\mu k_\nu}{\mathbf{k}^2} \right) \quad (16)$$

$$\mathcal{P}_{\mu\nu}^\parallel(k) = \left(\delta_{\mu\nu} - \frac{k_\mu k_\nu}{k^2} \right) - \mathcal{P}_{\mu\nu}^\perp(k_0, \mathbf{k}). \quad (17)$$

These projectors enjoy the usual properties $(\mathcal{P}^\perp)^2 = \mathcal{P}^\perp$ and $(\mathcal{P}^\parallel)^2 = \mathcal{P}^\parallel$, as well as $\mathcal{P}^\parallel \cdot \mathcal{P}^\perp = \mathcal{P}^\perp \cdot \mathcal{P}^\parallel = 0$; the traces in four euclidean dimensions are $\text{tr } \mathcal{P}^\perp = 2$ and $\text{tr } \mathcal{P}^\parallel = 1$. Obviously, $\mathcal{P}^\perp + \mathcal{P}^\parallel = \mathcal{P}$ is the usual 4-transversal projector.

Returning to the Gaussian trial measure eq. (8), we note that, for $\alpha = \frac{1}{2}$, the kernel ω equals the inverse gluon propagator and is thus subject to a Lorentz decomposition similar to eq. (15). For $\alpha \neq \frac{1}{2}$, the FP determinant \mathcal{J} contributes; below, we will treat \mathcal{J} in the so-called curvature approximation [35] which maintains the Lorentz structure of the kernel. As a consequence, the kernel must have the general form for all α ,

$$\omega_{\mu\nu}(k) = \omega_\perp(k) \cdot \mathcal{P}_{\mu\nu}^\perp(k) + \omega_\parallel(k) \cdot \mathcal{P}_{\mu\nu}^\parallel(k) + \gamma^{-1} k_\mu k_\nu, \quad (18)$$

where $\gamma = \zeta$ up to radiative corrections. The two scalar dressing functions ω_\perp and ω_\parallel depend on k_μ only through the two invariants k_0 and $|\mathbf{k}|$.

C. Curvature approximation and the ghost DSE

To complete our computational tools, we must also evaluate the FP determinant $\mathcal{J}(A)$ from eq. (11) and its expectation value in the trial measure (8). Unfortunately, this cannot be computed in closed form and we will resort to the finite-temperature equivalent of the so-called

³ To simplify the notation, we will often write $f(k)$ instead of $f(k_0, \mathbf{k})$ for a general function of the 4-momentum $k^\alpha = (k_0, \mathbf{k})$. If a function is $O(4)$ symmetric, $f(k)$ is really a scalar function of $k^2 \equiv k_0^2 + \mathbf{k}^2$; the distinction should always be clear from the context.

curvature approximation which was previously shown to be effective both in the Hamiltonian approach to Coulomb gauge [35], and in covariant gauges at zero temperatures [6]. In this approximation, the FP determinant is expressed as

$$\ln \mathcal{J}[A] \approx -\frac{1}{2} \int_{\beta} d(x, y) \chi_{\mu\nu}^{ab}(x, y) \cdot A_{\mu}^a(x) A_{\nu}^b(y), \quad (19)$$

where the *curvature* is given by the expectation value

$$\chi_{\mu\nu}^{ab}(x, y) \equiv - \left\langle \frac{\delta^2 \ln \mathcal{J}}{\delta A_{\mu}^a(x) \delta A_{\nu}^b(y)} \right\rangle \quad (20)$$

taken with the Gaussian measure eq. (8). From global colour invariance, we have again $\chi_{\mu\nu}^{ab} = \delta^{ab} \chi_{\mu\nu}$. Furthermore, the arguments put forward above to determine the Lorentz structure of the propagator also apply to the curvature. As a consequence, we have

$$\chi_{\mu\nu}(k) = \chi_{\perp}(k) \cdot \mathcal{P}_{\mu\nu}^{\perp}(k) + \chi_{\parallel}(k) \cdot \mathcal{P}_{\mu\nu}^{\parallel}(k) + \dots, \quad (21)$$

where the dots indicate irrelevant 4-longitudinal pieces which vanish in Landau gauge. We will derive integral equations for the profile functions in the next section.

If we put everything together, our *Ansatz* (8) for the trial measure becomes

$$d\mu(A) = \mathcal{N} \cdot \exp \left[-\frac{1}{2} \int_{\beta} \mathbf{d}k A_{\mu}^a(-k) \left\{ \bar{\omega}_{\perp}(k) \cdot \mathcal{P}_{\mu\nu}^{\perp}(k) + \bar{\omega}_{\parallel}(k) \cdot \mathcal{P}_{\mu\nu}^{\parallel}(k) + \bar{\tau}(k) \cdot k_{\mu} k_{\nu} \right\} \right], \quad (22)$$

where the profile functions are now

$$\begin{aligned} \bar{\omega}_{\perp} &\equiv \omega_{\perp} + (1 - 2\alpha) \chi_{\perp} \\ \bar{\omega}_{\parallel} &\equiv \omega_{\parallel} + (1 - 2\alpha) \chi_{\parallel}. \end{aligned} \quad (23)$$

A few remarks are in order at this point. Firstly, the full gluon propagator in our approach is

$$D_{\mu\nu}^{ab}(k) = \delta^{ab} \left[\bar{\omega}_{\perp}(k)^{-1} \cdot \mathcal{P}_{\mu\nu}^{\perp}(k) + \bar{\omega}_{\parallel}(k)^{-1} \cdot \mathcal{P}_{\mu\nu}^{\parallel}(k) + \bar{\tau}(k)^{-1} \cdot \frac{k_{\mu} k_{\nu}}{k^4} \right]. \quad (24)$$

The 4-longitudinal (last) piece in this expression is not very important and will even vanish in Landau gauge $\zeta \rightarrow 0$, which we will study exclusively below.

Secondly, the operator held fixed in our trial measure is not the gauge field itself, but rather the gluon propagator (cf. eq. (24)), i.e. according to the general setup explained in section II A, our variation principle optimizes the *effective action for the gluon propagator*. This is appropriate as long as we are not interested in higher vertices.

Finally, one might think that the curvature is irrelevant, as the final form of the trial measure including the FP determinant is still Gaussian. This is not so because the curvature reappears in the relative entropy $\overline{\mathcal{W}}$ that enters the free action.

D. The ghost sector

The ghost propagator is the expectation value of the inverse Faddeev-Popov operator which we decompose according to $G^{-1} \equiv -\partial_\mu \hat{D}_\mu = G_0^{-1} + h$, where

$$[G_0^{-1}]^{ab} = -\square \delta^{ab}, \quad h^{ab} = g f^{abc} \partial_\mu A_\mu^c \quad (25)$$

with the structure constants f^{abc} of the colour group $SU(N)$. From this, it is easy to see that the ghost propagator $\langle G \rangle$ satisfies the Dyson equation $\langle G \rangle^{-1} = G_0^{-1} + \langle hG \rangle \langle G \rangle^{-1}$. The expectation value $\langle hG \rangle$ involves the ghost-gluon Green's function, which in turn is obtained by attaching full propagators to the proper ghost-gluon vertex Γ_μ^{abc} . Using roman digits for the combination of Lorentz, colour and space-time indices, the ghost gluon vertex is defined by

$$\langle A(1) G(2,3) \rangle = -D(1,1') \langle G(2,2') \rangle \Gamma(2',3';1') \langle G(3'3) \rangle. \quad (26)$$

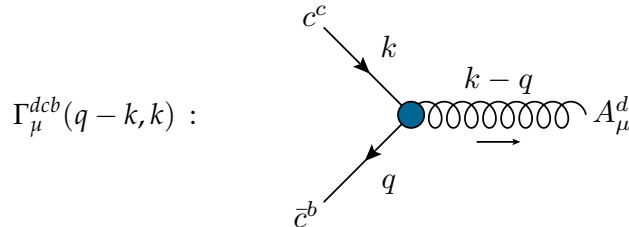
If we also introduce the *ghost form factor* $\eta(k)$ as the deviation of the full ghost propagator from the free one,

$$\langle G \rangle^{ab}(x,y) = \int_\beta \mathbf{d}k e^{ik \cdot (x-y)} \delta^{ab} \frac{\eta(k)}{k^2}, \quad (27)$$

we find the *exact* momentum space relation

$$\delta^{ab} \eta(k)^{-1} = \delta^{ab} + g f^{acd} \int_\beta \mathbf{d}q \frac{ik_\mu}{k^2} D_{\mu\nu}(q) \frac{\eta(k-q)}{(k-q)^2} \Gamma_\mu^{dcb}(q-k,k). \quad (28)$$

Here, we have used global colour invariance to deduce the colour structure $D_{\mu\nu}^{ab} = \delta^{ab} D_{\mu\nu}$ for the full gluon propagator, and the momentum routing in the vertex is



The exact eq. (28) is referred to as the ghost Dyson-Schwinger equation (DSE). In the *rainbow-ladder approximation*, the proper ghost-gluon vertex is replaced by the bare vertex defined by

$$\Gamma_0(2, 3; 1) = \frac{\delta G^{-1}(2, 3)}{\delta A(1)}, \quad (29)$$

which reads, with the momentum routing above,

$$[\Gamma_0]_\mu^{dcb}(q-k, k) \rightarrow ig f^{dcb} (q-k)_\mu. \quad (30)$$

The ladder approximation has been proven to be very reliable at $T = 0$ and we expect it to hold equally well at non-zero temperatures. From eq. (28), we then get a closed integral equation for the ghost form factor,

$$\eta(k)^{-1} = 1 - Ng^2 \int_\beta \mathbf{d}q \frac{\eta(k-q)}{(k-q)^2} \frac{k_\mu(k-q)_\nu D_{\mu\nu}(q)}{k^2}. \quad (31)$$

To complete the derivation of the ghost sector, we have to insert the gluon propagator eq. (18) from our Gaussian ansatz into eq. (31). This simplifies considerably in pure Landau gauge ($\zeta = 0$) when the gauge connection and the gluon propagator are 4-dimensionally transversal. From this point on, *we will therefore study Landau gauge ($\zeta = 0$) exclusively*. In this case, the ghost DSE (31) becomes

$$\begin{aligned} \eta(k)^{-1} = 1 - Ng^2 \int_\beta \mathbf{d}q \frac{\eta(k-q)}{(k-q)^2} \frac{1 - (\hat{\mathbf{k}} \cdot \hat{\mathbf{q}})^2}{\bar{\omega}_\parallel(q)} - \\ - Ng^2 \cdot \frac{\mathbf{k}^2}{k^2} \int_\beta \mathbf{d}q \frac{\eta(k-q)}{(k-q)^2} (1 - (\hat{\mathbf{k}} \cdot \hat{\mathbf{q}})^2) \left[\bar{\omega}_\perp(q)^{-1} - \bar{\omega}_\parallel(q)^{-1} \right], \end{aligned} \quad (32)$$

where $k^2 = k_0^2 + \mathbf{k}^2$ is the 4-momentum square and we have also introduced four- and three-dimensional unit vectors

$$\hat{k}_\mu = \frac{k_\mu}{\sqrt{k^2}}, \quad \hat{\mathbf{k}} = \frac{\mathbf{k}}{|\mathbf{k}|}. \quad (33)$$

Next, we concentrate on the curvature eq. (20). In our compact roman digits notation, we have

$$\chi(1, 2) = \text{Tr} \cdot \left\langle G \frac{\delta(-\partial\hat{D})}{\delta A(2)} \cdot G \cdot \frac{\delta(-\partial\hat{D})}{\delta A(1)} \right\rangle$$

The derivatives yield the bare ghost-gluon vertex Γ_0 (29), which is field-independent. To the given (formal) loop order, we therefore have $\langle G \Gamma_0 G \rangle \approx \langle G \rangle \Gamma_0 \langle G \rangle$. The remaining expectation values are merely the ghost propagators computed earlier. Restoring all arguments, we obtain the momentum space expression

$$\chi_{\mu\nu}^{ab}(k) = -\delta^{ab} Ng^2 \int_\beta \mathbf{d}q \frac{\eta(k-q)}{(k-q)^2} \frac{\eta(q)}{q^2} (k-q)_\mu q_\nu. \quad (34)$$

In Landau gauge, only the 4-transversal parts of this tensor contribute, which we find by contracting with the corresponding projectors \mathcal{P}^\perp and \mathcal{P}^\parallel , respectively. After some straightforward algebra, the profile functions in eq. (21) are

$$\begin{aligned}\chi_\perp(k) &= \frac{1}{2} N g^2 \int_\beta \mathfrak{d}q \frac{\eta(k-q) \eta(q)}{(k-q)^2} \frac{\mathbf{q}^2}{q^2} \left[1 - (\hat{\mathbf{k}} \cdot \hat{\mathbf{q}})^2 \right] \\ \chi_\parallel(k) &= N g^2 \int_\beta \mathfrak{d}q \frac{\eta(k-q) \eta(q)}{(k-q)^2} \left\{ 1 - (\hat{k} \cdot \hat{q})^2 - \frac{\mathbf{q}^2}{q^2} \left[1 - (\hat{\mathbf{k}} \cdot \hat{\mathbf{q}})^2 \right] \right\} .\end{aligned}\quad (35)$$

III. THE GAP EQUATION AT FINITE TEMPERATURES

A. The classical action

To derive the effective action for the gluon propagator, we must first evaluate the expectation value of the gauge-fixed YM action in the trial measure eq. (8),

$$\begin{aligned}\langle S_{\text{gf}} \rangle &= \frac{1}{2} \int_\beta dx \langle A_\mu^a(x) A_\nu^a(y) \rangle \left[-\square_x \delta_{\mu\nu} + (1 - \xi^{-1}) \partial_\mu^x \partial_\nu^x \right] \delta(x, y) + \\ &+ g f^{abc} \int_\beta dx \partial_\mu^x \langle A_\nu^a(x) A_\mu^b(x) A_\nu^c(x) \rangle + \frac{g^2}{4} f^{abc} f^{ade} \int_\beta dx \langle A_\mu^b(x) A_\nu^c(x) A_\mu^d(x) A_\nu^e(x) \rangle .\end{aligned}\quad (36)$$

The relevant correlators are easily evaluated using Wick's theorem, global colour invariance, and the $SU(N)$ relation $f^{abc} f^{abc} = N(N^2 - 1)$ to perform the colour traces. In momentum space, the result takes the form

$$\begin{aligned}\langle S_{\text{gf}} \rangle &= \frac{1}{2} (N^2 - 1) \beta V \int_\beta \mathfrak{d}k \left(k^2 \delta_{\mu\nu} - (1 - \zeta^{-1}) k_\mu k_\nu \right) D_{\mu\nu}(k) \\ &+ \frac{N g^2}{4} (N^2 - 1) \beta V \left[\int_\beta \mathfrak{d}k D_{\mu\mu}(k) \right]^2 - \frac{N g^2}{4} (N^2 - 1) \beta V \int_\beta \mathfrak{d}(k, q) D_{\mu\nu}(k) D_{\nu\mu}(q) ,\end{aligned}\quad (37)$$

where V is the 3-dimensional space volume. Next, we insert the representation (24) and take the Landau gauge limit $\zeta \rightarrow 0$ to find⁴

$$\begin{aligned} \frac{\langle S_{\text{gf}} \rangle}{(N^2 - 1) \beta V} = & \frac{1}{2} \int_{\beta} \mathbf{d}k k^2 \left[\frac{d-1}{\bar{\omega}_{\perp}(k)} + \frac{1}{\bar{\omega}_{\parallel}(k)} \right] + \frac{Ng^2}{4} \left\{ \int_{\beta} \mathbf{d}k \left[\frac{d-1}{\bar{\omega}_{\perp}(k)} + \frac{1}{\bar{\omega}_{\parallel}(k)} \right] \right\}^2 \\ & - \frac{Ng^2}{4} \int_{\beta} \mathbf{d}(k, q) \left\{ \frac{1 + (\hat{\mathbf{k}} \cdot \hat{\mathbf{q}})^2}{\bar{\omega}_{\perp}(k) \bar{\omega}_{\perp}(q)} + \frac{2}{\bar{\omega}_{\perp}(k) \bar{\omega}_{\parallel}(q)} (d-2 - (\hat{\mathbf{k}} \cdot \hat{\mathbf{q}})^2) \left(1 - \frac{\mathbf{q}^2}{q^2} \right) \right. \\ & \left. + \frac{1}{\bar{\omega}_{\parallel}(k) \bar{\omega}_{\parallel}(q)} \left[(\hat{k} \cdot \hat{q})^2 + (1 - (\hat{\mathbf{k}} \cdot \hat{\mathbf{q}})^2) \left(-1 + \frac{\mathbf{k}^2}{k^2} + \frac{\mathbf{q}^2}{q^2} \right) \right] \right\}. \quad (38) \end{aligned}$$

To further simplify this expression, we can exploit the remaining rotational symmetry to rewrite some of the integrals in which the integrand depends on $O(3)$ invariants only. After some straightforward but lengthy algebra, the classical action can be recast to

$$\begin{aligned} \langle S_{\text{gf}} \rangle = & \frac{1}{2} (N^2 - 1) \beta V \int_{\beta} \mathbf{d}q q^2 \left[\frac{2}{\bar{\omega}_{\perp}(q)} + \frac{1}{\bar{\omega}_{\parallel}(q)} \right] \\ & + \frac{1}{4} Ng^2 (N^2 - 1) \beta V \int_{\beta} \mathbf{d}(k, q) \left\{ \frac{A}{\bar{\omega}_{\perp}(k) \bar{\omega}_{\perp}(q)} + \frac{2B(q)}{\bar{\omega}_{\perp}(k) \bar{\omega}_{\parallel}(q)} + \frac{C(k, q)}{\bar{\omega}_{\parallel}(k) \bar{\omega}_{\parallel}(q)} \right\}, \quad (39) \end{aligned}$$

where the coefficients are given, for $d = 3$ space dimensions, by

$$\begin{aligned} A &= \frac{8}{3} \\ B(q) &= \frac{4}{3} + \frac{2}{3} \frac{\mathbf{q}^2}{q^2} \\ C(k, q) &= \frac{2}{3} + \frac{1}{3} \left(\frac{\mathbf{k}^2}{k^2} + \frac{\mathbf{q}^2}{q^2} \right) - \frac{4}{3} \frac{\mathbf{k}^2}{k^2} \frac{\mathbf{q}^2}{q^2}. \quad (40) \end{aligned}$$

B. The entropy

As the last ingredient, we need the relative entropy of the path integral measure (22) with respect to the Faddeev-Popov determinant. From eq. (7) and the curvature approximation

⁴ We have dropped the field- and temperature-independent constant

$$\frac{1}{2} \beta V (N^2 - 1) \int_{\beta} \mathbf{d}k = \frac{V}{2} (N^2 - 1) \sum_{n \in \mathbb{Z}} \int \frac{d^3 k}{(2\pi)^3}.$$

eq. (19), we obtain

$$\begin{aligned}
\overline{\mathcal{W}} &= \langle -\ln \rho \rangle + \langle \ln \mathcal{J} \rangle \\
&\approx -\ln \mathcal{N} + \frac{1}{2} \int_{\beta} d(x, y) \bar{\omega}_{\mu\nu}^{ab}(x, y) \langle A_{\mu}^a(x) A_{\nu}^b(y) \rangle - \frac{1}{2} \int_{\beta} d(x, y) \chi_{\mu\nu}^{ab}(x, y) \langle A_{\mu}^a(x) A_{\nu}^b(y) \rangle \\
&= -\ln \mathcal{N} + \frac{1}{2} \int_{\beta} d(x, y) \langle A_{\mu}^a(x) A_{\nu}^b(y) \rangle \left\{ \bar{\omega}_{\mu\nu}^{ab}(x, y) - \chi_{\mu\nu}^{ab}(x, y) \right\} \\
&= -\ln \det \left(\frac{2\pi}{\bar{\omega}} \right)^{-\frac{1}{2}} + \frac{1}{2} (N^2 - 1) \int_{\beta} d(x, y) \bar{\omega}_{\mu\nu}^{-1}(x, y) \left\{ \bar{\omega}_{\mu\nu}(x, y) - \chi_{\mu\nu}(x, y) \right\} \\
&= -\frac{1}{2} \text{Tr} \ln \left(\frac{\bar{\omega}_{\mu\nu}^{ab}}{2\pi} \right) + \frac{1}{2} (N^2 - 1) \beta V \int_{\beta} \mathbf{d}k \bar{\omega}_{\mu\nu}^{-1}(k) \left\{ \bar{\omega}_{\mu\nu}(k) - \chi_{\mu\nu}(k) \right\},
\end{aligned}$$

where the explicit form $\mathcal{N} = \det[\bar{\omega}/(2\pi)]^{\frac{1}{2}}$ for the normalisation in eq. (22) was used. In pure Landau gauge in three space dimensions, we have $\bar{\omega}_{\mu\nu}^{-1}(k) \bar{\omega}_{\mu\nu}(k) = \text{tr} \mathcal{P}(k) = 3$, where \mathcal{P} is the 4-transversal projector. Likewise,

$$\begin{aligned}
\bar{\omega}_{\mu\nu}^{-1}(k) \chi_{\mu\nu}(k) &= \bar{\omega}_{\perp}^{-1}(k) \chi_{\perp}(k) \cdot \text{tr} \mathcal{P}^{\perp}(k) + \bar{\omega}_{\parallel}^{-1}(k) \chi_{\parallel}(k) \cdot \text{tr} \mathcal{P}^{\parallel}(k) \\
&= 2 \bar{\omega}_{\perp}(k)^{-1} \chi_{\perp}(k) + \bar{\omega}_{\parallel}(k)^{-1} \chi_{\parallel}(k).
\end{aligned}$$

After dropping an irrelevant temperature- and field-independent term, the entropy becomes

$$\overline{\mathcal{W}} = -\frac{1}{2} (N^2 - 1) \text{Tr} \ln \left[\frac{\bar{\omega}_{\perp}}{2\pi} \mathcal{P}_{\mu\nu}^{\perp} + \frac{\bar{\omega}_{\parallel}}{2\pi} \mathcal{P}_{\mu\nu}^{\parallel} \right] - \frac{1}{2} (N^2 - 1) \beta V \int_{\beta} \mathbf{d}k \left\{ 2 \frac{\chi_{\perp}(k)}{\bar{\omega}_{\perp}(k)} + \frac{\chi_{\parallel}(k)}{\bar{\omega}_{\parallel}(k)} \right\}.$$

Since the projectors \mathcal{P}^{\perp} and \mathcal{P}^{\parallel} are orthogonal, the determinant in the first term factorizes. The dimensions of the subspaces on which \mathcal{P}^{\perp} and \mathcal{P}^{\parallel} project are 2 and 1, respectively, and in each subspace, the projector acts as unity. Expressing the functional trace in momentum space, we finally obtain

$$\overline{\mathcal{W}} = -\frac{1}{2} (N^2 - 1) \beta V \int_{\beta} \mathbf{d}k \left\{ 2 \ln \frac{\bar{\omega}_{\perp}(k)}{2\pi} + \ln \frac{\bar{\omega}_{\parallel}(k)}{2\pi} + 2 \frac{\chi(k)}{\bar{\omega}_{\perp}(k)} + \frac{\theta(k)}{\bar{\omega}_{\parallel}(k)} \right\}. \quad (41)$$

The difference of eqs. (39) and (41) is the effective action $\Gamma(\bar{\omega}_{\perp}, \bar{\omega}_{\parallel})$ for the (inverse) gluon propagator within the curvature approximation (19).

C. The gap equation

It is now straightforward to compute the optimal kernels (or gluon propagator) from the *gap equations*

$$\frac{\delta\Gamma(\bar{\omega}_\perp, \bar{\omega}_\parallel)}{\delta\bar{\omega}_\perp(k)} = \frac{\delta\Gamma(\bar{\omega}_\perp, \bar{\omega}_\parallel)}{\delta\bar{\omega}_\parallel(k)} = 0. \quad (42)$$

After more algebra, we obtain for the variation w.r.t $\bar{\omega}_\perp(k)$

$$0 = k^2 + \frac{1}{2}Ng^2 \int_\beta \mathbf{d}q \left[\frac{A}{\bar{\omega}_\perp(q)} + \frac{B(q)}{\bar{\omega}_\perp(q)} \right] - \bar{\omega}_\perp(k) + \chi_\perp(k) + \int_\beta \mathbf{d}q \frac{1}{\bar{\omega}_\perp(q)} \frac{\delta\chi(q)}{\delta\bar{\omega}_\perp(k)^{-1}}, \quad (43)$$

where the coefficients A and $B(q)$ are given in eq. (40). The curvature depends on $\bar{\omega}_\perp(q)$ through the ghost form factor η which enters eq. (35), but this is a higher loop effect that can safely be neglected within the curvature approximation. Dropping the last term in eq. (43), we arrive at

$$\bar{\omega}_\perp(k) = k_0^2 + \mathbf{k}^2 + \chi_\perp(k) + M_\perp^2(\beta) \quad (44)$$

$$M_\perp^2(\beta) \equiv \frac{1}{2}Ng^2 \int_\beta \mathbf{d}q \left[\frac{A}{\bar{\omega}_\perp(q)} + \frac{B(q)}{\bar{\omega}_\parallel(q)} \right]. \quad (45)$$

The second gap equation is derived in exactly the same fashion and takes the form

$$\bar{\omega}_\parallel(k) = k_0^2 + \mathbf{k}^2 + \chi_\parallel(k) + Ng^2 \int_\beta \mathbf{d}q \left[\frac{B(k)}{\bar{\omega}_\perp(q)} + \frac{C(k, q)}{\bar{\omega}_\parallel(q)} \right]. \quad (46)$$

In constrast to the previous case (45), the last piece has no direct interpretation as a mass term as it depends on the external momentum k_μ . However, at $\mathbf{k} = 0$ (with $k_0 \neq 0$), we find

$$Ng^2 \int_\beta \mathbf{d}q \left[\frac{B(k)}{\bar{\omega}_\perp(q)} + \frac{C(k, q)}{\bar{\omega}_\parallel(q)} \right] \xrightarrow{\mathbf{k}=0} M_\perp^2(\beta),$$

as can be shown by explicit calculation. We can thus factorize the momentum dependence in the last term on the rhs of eq. (46) and recast the second gap equation to

$$\bar{\omega}_\parallel(k) = k_0^2 + \mathbf{k}^2 + \chi_\parallel(k) + M_\perp^2(\beta) + \frac{\mathbf{k}^2}{k_0^2 + \mathbf{k}^2} \Delta M_\parallel^2(\beta) \quad (47)$$

$$\Delta M_\parallel^2(\beta) = \frac{1}{3}Ng^2 \int_\beta \mathbf{d}q \left[\frac{2}{\bar{\omega}_\perp(q)} + \left(\frac{q_0^2 - 3\mathbf{q}^2}{q_0^2 + \mathbf{q}^2} \right) \frac{1}{\bar{\omega}_\parallel(q)} \right]. \quad (48)$$

Eqs. (31), (35), (44) and (47) form a closed set of integral equations to determine the gluon and ghost propagators in Landau gauge at finite temperatures.

IV. RENORMALIZATION

Next we turn to the renormalization of our integral equation system. We expect that **(i)** the equations reduce to the known zero-temperature case in the limit $\beta \rightarrow \infty$ and **(ii)** the counterterms fixed in the zero-temperature limit are sufficient to renormalize the system at *any* temperature.

A. The zero temperature limit

Let us first study how the zero temperature limit formally arises in our integral equation system.⁵ The sum over Matsubara frequencies can generally be rewritten by Poisson resummation,

$$\frac{1}{\beta} \sum_{n=-\infty}^{\infty} f(\nu_n) = \int_{-\infty}^{\infty} \frac{dz}{2\pi} f(z) \sum_{m=-\infty}^{\infty} e^{im\beta z} = \sum_{m=-\infty}^{\infty} \tilde{f}(m\beta). \quad (49)$$

By the Riemann-Lebesgue lemma, the Fourier transform $\tilde{f}(x)$ vanishes at large arguments $|x| \rightarrow \infty$, i.e. only the term with $m = 0$ contributes in the zero-temperature limit,

$$\lim_{\beta \rightarrow \infty} \frac{1}{\beta} \sum_{n=-\infty}^{\infty} f(\nu_n) = \tilde{f}(0) = \int \frac{dp_0}{2\pi} f(p_0) \quad (50)$$

Let us assume for the moment that the ghost form factor $\eta(k)$ approaches the $O(4)$ -invariant zero-temperature form factor $\eta_0(k)$, cf. appendix A 1. (This assumption will be justified *a posteriori* below). From eq. (34) and the limit (50), we have

$$\chi_{\mu\nu}^{ab}(k) \xrightarrow{\beta \rightarrow \infty} -\delta^{ab} N g^2 \int \frac{d^4 q}{(2\pi)^4} \frac{\eta_0(k-q) \eta_0(q)}{(k-q)^2 q^2} (k-q)_\mu q_\nu.$$

Contracting with $\mathcal{P}_{\mu\nu}^\perp(k)$ gives

$$\lim_{\beta \rightarrow \infty} 2\chi_\perp(k) = -\delta^{ab} N g^2 \int \frac{d^4 q}{(2\pi)^4} \frac{\eta_0(k-q) \eta_0(q)}{(k-q)^2 q^2} (k-q)_\mu q_\nu \mathcal{P}_{\mu\nu}^\perp(k) = 2\chi_0(k),$$

where χ_0 is the zero-temperature curvature, cf. appendix A 1. From the second equation (35), it follows that $\chi_\parallel(k) \rightarrow 3\chi_0(k) - 2 \lim_{\beta \rightarrow \infty} \chi_\perp(k) = \chi_0(k)$ in the same limit and we have

$$\lim_{\beta \rightarrow \infty} \chi_\perp(k) = \lim_{\beta \rightarrow \infty} \chi_\parallel(k) = \chi_0(k). \quad (51)$$

⁵ Since we are dealing with the unrenormalized equations, an $O(3)$ invariant cutoff is implicitly assumed in this section.

In appendix A 2, it is further shown that the mass functions in the gap equation have the low-temperature limit $M_{\perp}^2(\beta) \rightarrow M_0^2$ and $\Delta M_{\parallel}^2(\beta) \rightarrow 0$. From eqs. (44), (47) and (51), it then follows immediately that

$$\lim_{\beta \rightarrow \infty} \bar{\omega}_{\perp}(k) = \lim_{\beta \rightarrow \infty} \bar{\omega}_{\parallel}(k) = k_0^2 + \mathbf{k}^2 + \chi_0(k) + M_0^2 = \bar{\omega}_0(k). \quad (52)$$

Finally, this relation shows that the second line in eq. (32) vanishes as $\beta \rightarrow \infty$, while the first line approaches $\eta_0(k)$ as can be seen from eqs. (A1) and (A2). Thus, the self-consistent solution has also

$$\lim_{\beta \rightarrow \infty} \eta(k) = \eta_0(k), \quad (53)$$

which justifies our initial assumption above. Altogether, eqs. (51)-(53) are the expected $\beta \rightarrow \infty$ limit in which the full $O(4)$ symmetry is restored.

B. Renormalization at zero temperature

In this section, we recall (and simplify) the renormalization of the zero temperature system as layed out in Ref. [6]. This information is required later on, since we must fix all counter terms at zero temperature in order to compare different temperature settings reliably. After introducing ghost fields c, \bar{c} to make the Faddeev-Popov determinant local, three counter terms are required,

$$\mathcal{L}_{\text{ct}} = \delta Z_A \cdot \frac{1}{4} (\partial_{\mu} A_{\nu}^a - \partial_{\nu} A_{\mu}^a)^2 + \delta M^2 \cdot \frac{1}{2} (A_{\mu}^a)^2 + \delta Z_c \cdot \partial_{\mu} \bar{c} \partial^{\mu} c \quad (54)$$

corresponding to a gluon wave function, gluon mass, and ghost field renormalisation. (No vertex renormalisation is induced by the theory.) The counterterms $\int d^4x \mathcal{L}_{\text{ct}}$ must be added to the exponent of the (Gaussian) trial measure eq. (8) used to compute the n -point functions, i.e. they are *not* counterterms to the Yang-Mills action directly. The renormalized integral equation system at zero temperature then becomes

$$\begin{aligned} \bar{\omega}_0(k) &= k^2 + M_0^2 + \chi_0(k) & M_0^2 &= Ng^2 I_M^{(0)} + \delta M_1^2 \\ \eta_0(k)^{-1} &= 1 - Ng^2 I_{\eta}^{(0)}(k) - \delta Z_c & \chi_0(k) &= Ng^2 I_{\chi}^{(0)}(k) + \delta\chi + k^2 \delta Z_A, \end{aligned} \quad (55)$$

where the explicit form of the various loop integrals is listed in appendix A 1. The mass counterterm has been split, $\delta M^2 = \delta M_1^2 + \delta\chi$, between the mass and the curvature since only the sum of these contributions enters the gap equation (55).

As layed out in Ref. [6], we have to choose slightly unusual renormalization conditions to overcome numerical problems in the deep infrared. Normally, one would prescribe the value of the propagators and vertices at a common (large) scale $\mu \gg 1$, except for the mass counterterm which determines the propagator at zero momentum (in Euclidean space). In the present case, we impose the value of the *ghost propagator*, or ghost form factor $\eta(\mu_c)$, at a low scale $\mu_c \ll 1$ (which could even be taken to be $\mu_c = 0$) in order to discern the scaling from the decoupling solution [6]; this condition determines the counter term

$$\delta Z_c = 1 - Ng^2 I_\eta^{(0)}(\mu_c) - \eta_0(\mu_c)^{-1}. \quad (56)$$

The remaining renormalization conditions for the gluon can be taken conventionally: we impose the value of the (inverse) propagator at a large scale $\mu \gg 1$ to fix the field renormalisation δZ_A , and at a small scale $\mu_0 \ll 1$ to fix the mass counterterm⁶,

$$\bar{\omega}_0(\mu) =: Z \mu^2, \quad \bar{\omega}_0(\mu_0) =: Z M_A^2. \quad (57)$$

For later reference, we note the explicit form of the counterterm coefficients⁷

$$\begin{aligned} 1 + \delta Z_A &= Z \frac{\mu^2 - M_A^2}{\mu^2 - \mu_0^2} - Ng^2 \frac{I_\chi^{(0)}(\mu) - I_\chi^{(0)}(\mu_0)}{\mu^2 - \mu_0^2} \\ M_0^2 + \delta M^2 &= Z \mu^2 \frac{M_A^2 - \mu_0^2}{\mu^2 - \mu_0^2} - Ng^2 \frac{\mu^2 I_\chi^{(0)}(\mu_0) - \mu_0^2 I_\chi^{(0)}(\mu)}{\mu^2 - \mu_0^2}, \end{aligned} \quad (58)$$

which complement eq. (56) in the ghost sector. With these conditions, the renormalized integral equation system at zero temperature becomes⁸

$$\begin{aligned} \eta_0(k)^{-1} &= \eta_0(\mu_c)^{-1} - Ng^2 \left[I_\eta^{(0)}(k) - I_\eta^{(0)}(\mu_c) \right] \\ \bar{\omega}_0(k) &= Z \frac{\mu^2 - M_A^2}{\mu^2 - \mu_0^2} k^2 + Z \frac{M_A^2 - \mu_0^2}{\mu^2 - \mu_0^2} \mu^2 + \frac{Ng^2}{\mu^2 - \mu_0^2} \left[\mu^2 (I_\chi^{(0)}(k) - I_\chi^{(0)}(\mu_0)) - \right. \\ &\quad \left. - k^2 (I_\chi^{(0)}(\mu) - I_\chi^{(0)}(\mu_0)) - \mu_0^2 (I_\chi^{(0)}(k) - I_\chi^{(0)}(\mu)) \right]. \end{aligned} \quad (59)$$

Note that the difference of integrals in the square brackets is finite: For the first equation (59), this is clear because $I_\eta^{(0)}$ is logarithmically UV divergent by power counting. In the second

⁶ For the decoupling solution, we could choose $\mu_0 \rightarrow 0$ so that M_A^2 could be interpreted as a constituent gluon mass; in the general case, however, we must take $\mu_0 > 0$ to avoid infrared singularities, and M_A^2 becomes a general mass parameter.

⁷ The symbol Z should not be confused with the gluon field renormalization constant, which is $Z_A = 1 + \delta Z_A$.

⁸ The finite parts in the ghost counter term δZ_c are such that the first equation in (59) could also be obtained by simply subtracting the bare ghost DSE for $\eta_0(k)$ at the renormalization scale μ_c .

equation (59), $I_\chi^{(0)}$ is quadratically divergent, but the subleading logarithmic divergence is also eliminated due to the clever combination of $I_\chi^{(0)}$ at three different scales.

The system eq. (59) is well suited for a numerical evaluation. It contains, besides the three renormalization constants $\{\eta_0(\mu_c), Z, M_A^2\}$, also the coupling strength⁹ in the combination Ng^2 . However, this parameter is *redundant*. To see this, consider a solution $\bar{\omega}_0(k)$, $\eta_0(k)$ of eq. (59) obtained with a set of parameters $\{\eta_0(\mu_c), Z, M_A^2, Ng^2\}$. From the form of the loop integrals in eq. (59) listed in appendix A 3, it is apparent that the rescaled parameters

$$\{\eta_0(\mu_c), Z, M_A^2, Ng^2\} \rightarrow \{a \cdot \eta_0(\mu_c), b \cdot Z, M_A^2, b/a^2 \cdot Ng^2\} \quad (60)$$

lead to the solution $a \eta_0(k)$ and $b \bar{\omega}_0(k)$, in which the propagators are scaled by arbitrary factors. Thus, any change in Ng^2 can be compensated by a corresponding rescaling of the propagators (and vice versa), including their field renormalisation constants $\eta_0(\mu_c)$ and Z . We can thus *choose* to set $Ng^2 = 1$ in eq. (59), with the provision that the propagators (and their field renormalization constants) may later be multiplied by an overall constant when fitting to lattice data. The solution of eq. (59) therefore depends on the three renormalization constants $\{\eta_0(\mu_c), Z, M_A^2\}$ only, where the first two determine the overall scale of the propagators, while M_A^2 determines the behaviour in the intermediate momentum region. Formally, M_A^2 can be chosen arbitrarily, but it is related through a gap equation to the gluon propagator and the bare Mass M_0 . Since this gap equation involves Ng^2 , different colour groups $SU(N)$ will require, in general, different value for M_A^2 . For the case of $SU(2)$, we will give a numerical estimate for M_A^2 from high-precision lattice data in section V A below.

C. Renormalization at finite temperatures

Next we turn to the integral equation system at finite temperatures. In the previous section, the counter terms were constructed at zero temperature and it is important to use the *same* counter terms also at non-zero temperatures in order to compare different temperatures reliably. To do so, we merely have to add $(-\delta Z_c)$ from eq. (56) to the right hand side of eq. (32), and likewise $(\delta Z_A k^2 + \delta M^2)$ from eq. (58) to the right hand side of eqs. (44) and (47). The resulting system of equations can be written in two equivalent forms. This is best demonstrated

⁹ In the present approximation scheme, Ng^2 is a finite adjustable parameter since there are no vertex corrections.

at the ghost equation:

$$\begin{aligned}
\eta(k)^{-1} &= 1 - Ng^2 I_\eta(k) - Ng^2 \frac{\mathbf{k}^2}{k^2} \underbrace{\int_\beta \mathbf{d}q \frac{\eta(k-q)}{(k-q)^2} \left[1 - (\hat{\mathbf{k}} \cdot \hat{\mathbf{q}})^2\right] \left[\bar{\omega}_\perp(q)^{-1} - \bar{\omega}_\parallel(q)^{-1}\right]}_{\equiv L_\eta(k)} - \delta Z_c \\
&= 1 - Ng^2 I_\eta(k) - Ng^2 \frac{\mathbf{k}^2}{k^2} L_\eta(k) - \left[1 - Ng^2 I_\eta^{(0)}(\mu_c) - \eta_0(\mu_c)^{-1}\right] \\
&= \eta_0(\mu_c)^{-1} - Ng^2 \left[I_\eta(k) - I_\eta^{(0)}(\mu_c)\right] - Ng^2 \frac{\mathbf{k}^2}{k^2} L_\eta(k) \\
&= \eta_0(k)^{-1} - Ng^2 \left[I_\eta(k) - I_\eta^{(0)}(k)\right] - Ng^2 \frac{\mathbf{k}^2}{k^2} L_\eta(k), \tag{61}
\end{aligned}$$

where the zero temperature equation (59) was used in the last step. The advantage of this formulation is that it avoids all explicit renormalization factors, as the finite temperature solution is expressed as its zero temperature counterpart plus a temperature-dependent correction which must be finite as all counterterms have already been consumed in $\eta_0(k)$. To confirm this, we note that the curvature and mass term in the gap equations (44), (47) are subdominant, which implies that $|\bar{\omega}_\perp(k)^{-1} - \bar{\omega}_\parallel(k)^{-1}| \sim \mathcal{O}(k^{-4})$ at large momenta and $L_\eta(k)$ is finite by power counting. As for the difference $I_\eta(k) - I_\eta^{(0)}(k)$ of logarithmically divergent loop integrals, we note that this would be finite at *zero temperature*. At nonzero temperature, however, this statement is less obvious, since $I_\eta(k)$ and $I_\eta^{(0)}(k)$ involve different form factors in their integrand. In principle, the restoration of $O(4)$ invariance at large momenta should ensure that the difference is finite at any temperature, but this limit is very hard to reach *numerically*. We will therefore follow a different route in our numerical investigation below.

Similar considerations can also be applied to the gap equation. After some algebra, we obtain

$$\begin{aligned}
\eta(k_0, |\mathbf{k}|)^{-1} &= \eta_0(k)^{-1} - Ng^2 \left[I_\eta(k_0, |\mathbf{k}|) - I_\eta^{(0)}(k)\right] - \frac{\mathbf{k}^2}{k_0^2 + \mathbf{k}^2} Ng^2 L_\eta(k_0, |\mathbf{k}|) \\
\bar{\omega}_\perp(k_0, |\mathbf{k}|) &= \bar{\omega}_0(k) + Ng^2 \left[I_\chi^\perp(k_0, |\mathbf{k}|) - I_\chi^{(0)}(k)\right] + \left[M_\perp^2(\beta) - M_0^2\right] \\
\bar{\omega}_\parallel(k_0, |\mathbf{k}|) &= \bar{\omega}_0(k) + Ng^2 \left[I_\chi^\parallel(k_0, |\mathbf{k}|) - I_\chi^{(0)}(k)\right] + \left[M_\perp^2(\beta) - M_0^2\right] + \frac{\mathbf{k}^2}{k_0^2 + \mathbf{k}^2} \Delta M_\parallel^2(\beta). \tag{62}
\end{aligned}$$

To avoid confusion, we have reinserted to full momentum dependence in the finite-temperature profiles and loop integrals. Explicit expressions for the loop integrals entering this system can be found in appendix A 3.

As mentioned above, the system eq. (62) is hard to treat *numerically* because the difference of loop integrals involve non-zero and zero temperature form factors, respectively. We will

therefore rewrite these equations to bring them as close as possible to the zero-temperature case. Let us again consider the ghost equation as an example. From the second line in eq. (61), we have

$$\eta(k_0, |\mathbf{k}|)^{-1} = \eta(0, \mu_c)^{-1} - Ng^2 \left[I_\eta(k_0, |\mathbf{k}|) - I_\eta(0, \mu_c) \right] - Ng^2 \left[\frac{\mathbf{k}^2}{k_0^2 + \mathbf{k}^2} L_\eta(k_0, |\mathbf{k}|) - L_\eta(0, \mu_c) \right]$$

Here, we have chosen the renormalization point at vanishing Matsubara frequency.¹⁰ The benefit of this reformulation is that it only involves the difference of *the same* finite-temperature loop integrals (with the same form factors) at different scales. The cumbersome difference of loop integrals with different profiles is now hidden in a single number, namely the (finite) value of the form factor at the renormalization scale,

$$\eta(0, \mu_c)^{-1} = \eta_0(\mu_c)^{-1} - \left[I_\eta(0, \mu_c) - I_\eta^{(0)}(\mu_c) - L_\eta(0, \mu_c) \right]. \quad (63)$$

Again, we cannot compute this quantity reliably due to numerical issues, and we cannot choose it arbitrarily either, as it is determined completely by the zero-temperature counter terms. We will instead fix $\eta(0, \mu_c)$ indirectly as explained in detail in section VB below.

The gap equations can be rewritten in much the same way. After some lengthy algebra, we

¹⁰ The orientation of the renormalization point in 3-space is arbitrary due to the residual rotation symmetry, and we can choose the same direction as the external momentum, $(0, \mu_c \cdot \hat{\mathbf{k}})$, if this is ever necessary. A similar statement applies to the other two renormalization scales μ_0 and μ .

arrive at the following system:

$$\begin{aligned}
\eta(k_0, k)^{-1} &= \eta(0, \mu_c)^{-1} - Ng^2 \left[I_\eta(k_0, k) - I_\eta(0, \mu_c) \right] - Ng^2 \left[\frac{k^2}{k_0^2 + k^2} L_\eta(k_0, k) - L_\eta(0, \mu_c) \right] \\
\bar{\omega}_\perp(k_0, k) &= \bar{\omega}_\perp(0, \mu) + \frac{\mu^2 - (k_0^2 + k^2)}{\mu^2 - \mu_0^2} \left[\bar{\omega}_\perp(0, \mu_0) - \bar{\omega}_\perp(0, \mu) \right] + \\
&\quad + \frac{Ng^2}{\mu^2 - \mu_0^2} \left\{ \mu^2 \left[I_\chi^\perp(k_0, k) - I_\chi^\perp(0, \mu_0) \right] - (k_0^2 + k^2) \left[I_\chi^\perp(0, \mu) - I_\chi^\perp(0, \mu_0) \right] \right. \\
&\quad \left. - \mu_0^2 \left[I_\chi^\perp(k_0, k) - I_\chi^\perp(0, \mu) \right] \right\} \\
\bar{\omega}_\parallel(k_0, k) &= \bar{\omega}_\parallel(0, \mu) + \frac{\mu^2 - (k_0^2 + k^2)}{\mu^2 - \mu_0^2} \left[\bar{\omega}_\parallel(0, \mu_0) - \bar{\omega}_\parallel(0, \mu) \right] - \frac{k_0^2}{k_0^2 + k^2} \Delta M_\parallel^2(\beta) + \\
&\quad + \frac{Ng^2}{\mu^2 - \mu_0^2} \left\{ \mu^2 \left[I_\chi^\parallel(k_0, k) - I_\chi^\parallel(0, \mu_0) \right] - (k_0^2 + k^2) \left[I_\chi^\parallel(0, \mu) - I_\chi^\parallel(0, \mu_0) \right] \right. \\
&\quad \left. - \mu_0^2 \left[I_\chi^\parallel(k_0, k) - I_\chi^\parallel(0, \mu) \right] \right\}. \tag{64}
\end{aligned}$$

Here, $k = |\mathbf{k}|$ and we have spelled out all arguments to the loop integrals for clarity. The gap equations now exhibit the same combination of curvature integrals at three different scales which eliminated all divergences in the zero-temperature case. Alltogether, eq. (64) contains, in addition to the coupling constant Ng^2 , five temperature-dependent constants,

$$\bar{\omega}_\perp(0, \mu_0), \quad \bar{\omega}_\perp(0, \mu_0), \quad \bar{\omega}_\parallel(0, \mu_0), \quad \bar{\omega}_\parallel(0, \mu_0), \quad \eta(0, \mu_c), \tag{65}$$

which are all determined, in principle, by the zero-temperature counter terms through finite equations that are, however, hard to treat numerically. For completeness, these relations are listed in appendix A 4, although we will not use them and determine the constants in eq. (65) indirectly by other means.

The systems (62) and (64) are the main result of this paper. In the next chapter, we will give details on its numerical implementation and discuss the solutions.

V. NUMERICAL TREATMENT AND RESULTS

A. Renormalization at zero temperature

As explained in the last section, the renormalization of our approach must be carried out entirely at zero temperature. In section IV B, we have presented a simplified procedure, where all counter terms are determined by simple local prescriptions to low order Green's functions. Since this is different from the procedure initially laid out in Ref. [6], we cannot directly take over those results and must first re-determine the optimal renormalization parameters to match the known lattice results. This is carried out at zero temperature, and we take again the high-precision $SU(2)$ lattice data from Ref. [13].

In figure 1, we compare the best fit of our zero-temperature formulation to the lattice data for both the gluon propagator and the ghost form factor. Since we already know that the physically realized solution is *subcritical* (decoupling solution), only this type of solution is investigated. The scale μ_0 for the gluon mass renormalization could thus be taken to zero, but it is numerically favourable to impose this condition at a small but non-zero scale $\mu_0 \approx \mu/10$. As can be seen, the new renormalization prescription describes the lattice data with similar (high) precision as the more complicated prescription in Ref. [6]. We find $M_A/\mu \approx 0.49$ at $\mu \approx 1$ GeV to be a favourable parameter, but this determination has rather great uncertainties. As can be seen from figure 1, this is not because the approach could not describe the data, but rather since different combinations of the renormalization constants produce similar results, i.e. there are (almost) flat directions in renormalization space. From the comparison to the lattice data, we can also determine our parameters in absolute numbers. For the choice in figure 1, we can match the data at the point $\mu = 0.96$ GeV, where we find

$$M_A \approx 0.48 \text{ GeV} . \tag{66}$$

The renormalization scale μ is, of course, arbitrary as long as it is sufficiently deep in the ultraviolet. To check this, we have re-determined the renormalization parameters when matching at the larger scale $\mu = 5$ GeV. The best match to the lattice data in this case is virtually undistinguishable from figure 1. The renormalization parameters change considerably and, in particular, we now have $M_A/\mu \approx 0.173$, which again yields eq. (66) in physical units. In this sense, the mass parameter M_A is invariant under the renormalization group.

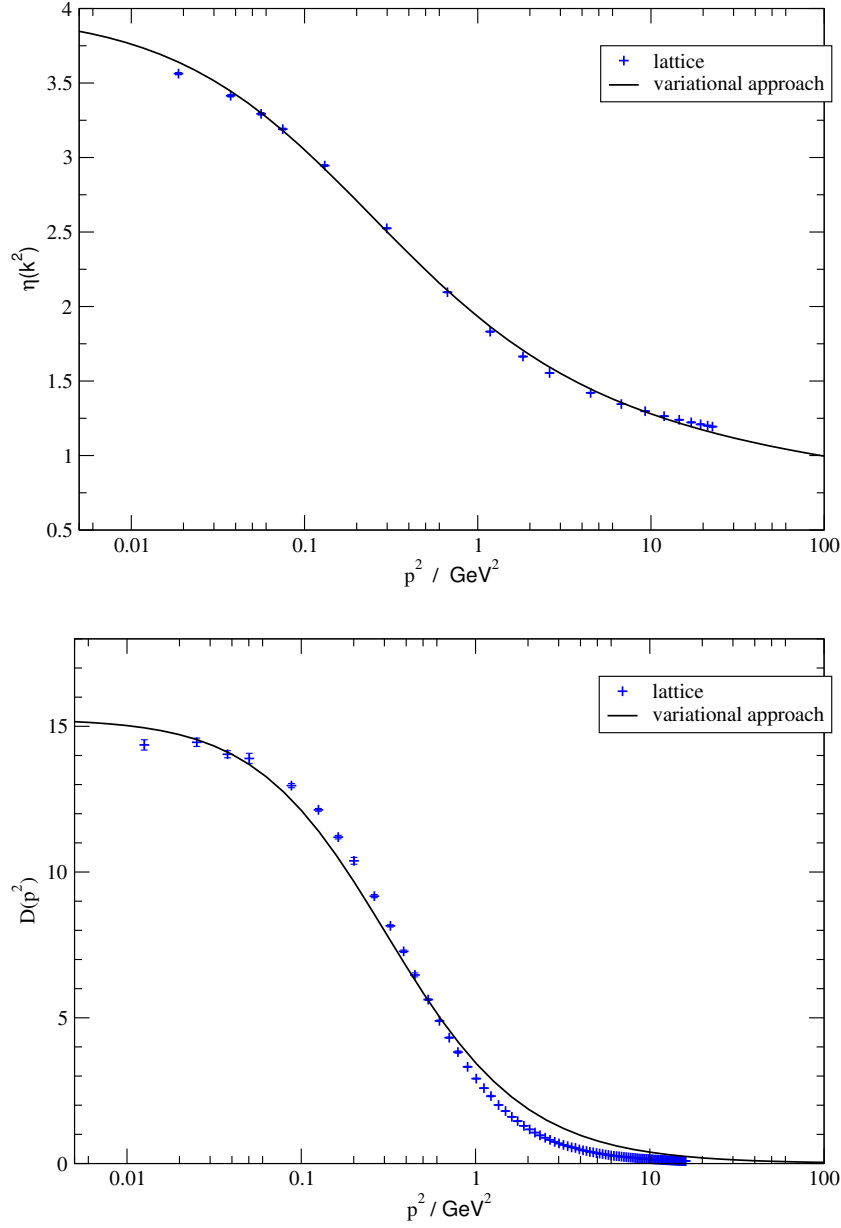


FIG. 1. The ghost form factor $\eta(p^2)$ (*top*) and the gluon propagator $D(p^2)$ (*bottom*) in Landau gauge at zero temperature. Lattice data is taken from Ref. [13], and the gluon mass renormalization parameter is $M_A \approx 0.48 \text{ GeV}$.

It must be emphasized, however, that the determination of the absolute scales is not very accurate and different values may produce similar results as in figure 1. Ultimately, the scales should be fixed by the comparison to the string tension computed from the effective action for the *Polyakov loop*, which is currently under investigation.

B. Numerical procedure at finite temperature

At finite temperature, our numerical procedure is based on eq. (64). The five constants eq. (65) entering this system are, in principle, fixed through the zero-temperature counter terms $\eta_0(\mu_c)$, Z and M_A . The first two of these three parameters only adjust the overall normalization of the zero-temperature propagators, which in turn fix the normalization of the finite-temperature propagators as well. In practice, the field normalization is rarely expressed through the zero-temperature counter terms, but rather by the alternative condition that the propagators at *all* temperatures should pass through the same point at a very large scale ,

$$\bar{\omega}_\perp(0, \mu_\infty) = \bar{\omega}_\parallel(0, \mu_\infty) = Z \mu_\infty^2, \quad \mu_\infty \gg 1. \quad (67)$$

This is based on the idea that finite temperature effects should become immaterial in the deep perturbative region where $O(4)$ invariance is restored. The lattice study in Ref. [41], to which we compare, employs a similar prescription with $\mu_\infty = 5 \text{ GeV}$. If we adopt eq. (66), this means $\mu_\infty \approx 5\mu$, but much larger values are also accessible in our case. In any case, the prescription eq. (67) can be imposed simply by replacing $\mu \rightarrow \mu_\infty$ in the second and third eq. (64). The values at the reference scale, $\bar{\omega}_\perp(0, \mu)$ and $\bar{\omega}_\parallel(0, \mu)$ are then temperature-dependent *predictions* of the calculation, which should agree with the results of the more complicated approach A 4 if the scale μ_∞ is chosen large enough. This reasoning allows us to compare to lattice data conveniently, and to determine the two constants $\bar{\omega}_\perp(0, \mu)$ and $\bar{\omega}_\parallel(0, \mu)$ in eq. (64) self-consistently.

For the ghost form factor, we would like to use the same procedure but this is hampered by the fact that we *must* impose a boundary condition in the deep infra-red in order to discern scaling and decoupling types of solution. This means that we have to *guess* the (temperature-dependent) intercept $\eta(0, \mu_c)$ at $\mu_c \approx 0$ such that the solution passes through the common value

$$\eta(0, \mu_\infty) = Z_c \quad (68)$$

for all temperatures. This leaves us with the remaining mass terms

$$\bar{\omega}_\perp(0, \mu_0) = Z m_\perp^2, \quad \bar{\omega}_\parallel(0, \mu_0) = Z m_\parallel^2, \quad \Delta M_\parallel^2 = Z \Delta m_\parallel^2. \quad (69)$$

which cannot be determined self-consistently by any scaling procedure, as they are not related to field renormalizations. We will determine them by fitting to the lattice data, i.e. we

have three parameters to cover the entire momentum range for all three propagators at each temperature. The need to fit eq. (69) (when we actually have equations to compute them) is only due to numerical issues. We can, however, take the alternative point of view that the coefficients eq. (69) are part of our variational ansatz (which includes the renormalization procedure), and the fit corresponds to a solution of the corresponding gap-equation. This is very much in line with the general philosophy of our approach, although it would, of course, be desirable to compute eq. (69) self-consistently without input from the lattice.

It should also be mentioned that the mass parameter ΔM_{\parallel}^2 could actually be computed from eq. (A5). We have still included it in the set of fit parameters, because eq. (A5) as well as the full dynamical system eq. (64) contains the coupling constant Ng^2 . From eq. (64) and the explicit form of the loop integrals, it is apparent that the factors of Ng^2 could be eliminated by the same scaling procedure that we used in the case of zero temperature. However, Ng^2 is temperature-independent, and so, only temperature-independent norm changes (rescalings) of the propagators are allowed. In addition, such rescalings do not leave the mass coefficients in eq. (69) invariant. This means that all three mass coefficients must be *fitted* to lattice data (or ideally determined from appendix A 4) if we rescale the propagators or change Ng^2 . In particular, the mass coefficients eq. (69) must be re-determined if we change the colour group $SU(N)$. The bottom line is that we are entitled to **(i)** set $Ng^2 = 1$, **(ii)** re-determine the coefficients in eq. (69) for each temperature and **(iii)** allow for temperature-independent rescalings of the propagators. Since the mass parameter Δm_{\parallel} has negligible influence on the final result, we will always set $\Delta m_{\parallel} = 0$. Then, the entire system has only two free parameters, m_{\perp} and m_{\parallel} , at each temperature, in addition to a temperature-independent overall norm scale for each form factor.

Numerically, the main issue in eq. (64) as compared to the zero-temperature case is the appearance of the Matsubara sum which replaces the frequency integral. There are various techniques to compute this sum. A direct evaluation is hampered by the fact that only a relatively small number of frequencies can be included in the coupled integral equation system to keep the overall computational effort under control. Typically, we include up to $n_{\max} \approx 20$ frequencies which corresponds, at a typical temperature $\mu\beta \approx 1$, to a frequency cutoff of $2\pi n_{\max}/\beta \approx 130\mu$ which is much smaller than the spatial momentum cutoff $\Lambda/\mu = O(10^5)$. Whether or not this is sufficient depends on the temperature itself: At high temperatures, the

Matsubara sum converges quickly and summing n_{\max} frequencies is sufficient. At lower temperatures, more frequencies contribute and we have to resort to more elaborate summation techniques as explained below.

C. Cutoff independence

Before presenting our numerical results, we must ensure that the finite-temperature system eq. (64) is indeed cutoff-independent. We must show this for both the momentum and frequency cutoff independently, and for all components of the solution at various temperatures. This gives a bewildering number of plots and we only present two representative cases, the remaining ones all displaying the same behaviour.

Since the cutoff-dependence can be studied at each temperature independently, we do not need to guess the correct ghost intercept $\eta(0, \mu_c)$ to ensure eq. (68) at all temperatures. Instead, we take an arbitrary fixed value $\eta(0, \mu_c) = 14$ at $\mu_c = 0$. The gluon normalization is fixed at $\mu_\infty = 4\mu$ with $Z = 0.8$ and for the mass parameters, we take $m_\perp = m_\parallel = M_A \approx 0.5\mu$ at $\mu_0 = \mu/10$ (and $\Delta m_\parallel = 0$). With this setup, we study the ghost form factor $\eta(k_0, |\mathbf{k}|)$ as a function of the spatial momentum $k = |\mathbf{k}|$, at vanishing Matsubara frequency $k_0 = 0$.¹¹ We vary both the frequency and momentum cutoff, at various temperatures, and check how this affects the results.

In table I, we show the dependence of the ghost form factor on the spatial cutoff Λ for two typical temperatures $\beta = 0.5/\mu$ and $\beta = 20.0/\mu$. We have fixed the number of Matsubara frequencies to $n_{\max} = 20$ and perform the frequency sum naively without further extrapolation. (We will see below that this is sufficient for these temperatures.) As can be clearly seen, the dependence on the spatial momentum cutoff Λ is almost negligible. The sensitivity is slightly more pronounced for the lower of the two temperatures, and for larger external momenta $k = |\mathbf{k}|$. In both cases, the maximal change of the ghost form factor $\eta(0, k)$ observed at $k = 10\mu$ is less than 4% when varying Λ by three orders of magnitude. This clearly indicates that both the quadratic *and* logarithmic divergences have been removed in our formulation eq. (64), and that the perturbative region sets in fairly quickly, even below $\Lambda = 10\mu$.

For the Matsubara sum, the situation is slightly more complicated. In general, the loop contributions from the Matsubara frequency $\#n$, after integrating over angles and spatial loop

¹¹ Higher Matsubara frequencies $k_0 > 0$ show the same behaviour.

	$k = 0.01$	$k = 0.05$	$k = 0.1$	$k = 0.5$	$k = 1.0$	$k = 5.0$	$k = 10.0$
$\Lambda = 1$	11.03	6.30	4.41	1.88	1.51		
$\Lambda = 10$	11.03	6.30	4.41	1.88	1.50	1.25	1.22
$\Lambda = 100$	11.03	6.30	4.41	1.87	1.50	1.24	1.21
$\Lambda = 10000$	11.01	6.28	4.41	1.88	1.51	2.25	1.22
$\Lambda = 1$	13.82	13.09	12.33	9.09	7.69		
$\Lambda = 10$	13.82	13.09	12.33	9.12	7.65	5.53	5.00
$\Lambda = 100$	13.82	13.09	12.34	9.21	7.82	5.72	5.19
$\Lambda = 10000$	13.82	13.09	12.34	9.20	7.78	5.68	5.20

TABLE I. Dependence of the ghost form factor $\eta(0, k)$ on the spatial momentum cutoff Λ . The upper table is for $\beta = 0.5$, the lower one for $\beta = 20.0$. All dimensionfull quantities are measured in units of the renormalization scale μ .

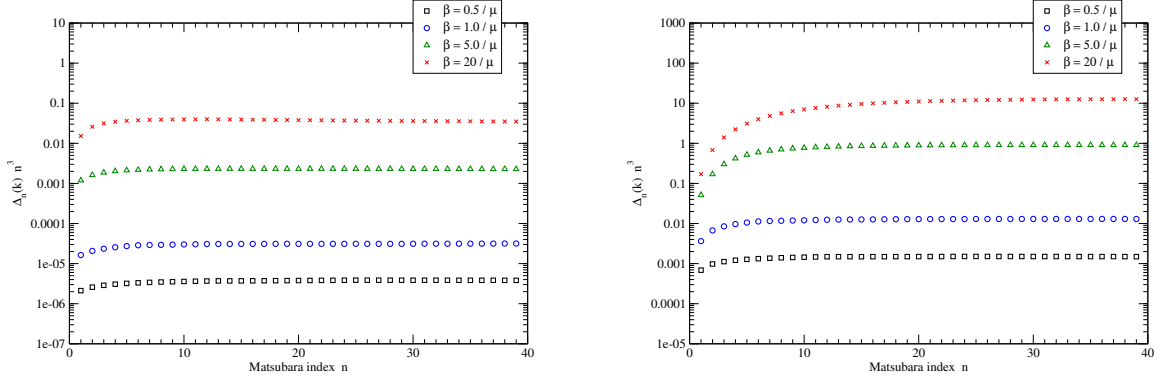


FIG. 2. The contribution $\Delta_n(k)$ of the n 'th Matsubara mode to the gluon form factor $\eta(0, k)$ at external momentum k . The left panel shows data for $k = 0.5 \mu$ and various temperatures on a logarithmic plot, while the right panel shows the same for $k = 10 \mu$. The contributions are multiplied by n^3 to better show their asymptotics.

momentum, decay as $1/n^3$ asymptotically, which leads to a convergent Matsubara sum.¹² To demonstrate this behaviour, let us consider the loop contribution $\Delta_n(k)$ to the ghost form

¹² Our counting is such that $n \geq 0$ and contributions with $n \neq 0$ are actually the sum of n and $(-n)$, which are equal in the present case.

factor from the first line in eq. (64),

$$\begin{aligned}\eta(0, k)^{-1} - \eta(0, \mu_c)^{-1} &= \left[I_\eta(0, \mu_c) - I_\eta(0, k) \right] - \left[L_\eta(0, \mu_c) - L_\eta(0, k) \right] \\ &\equiv \beta^{-1} \sum_{n=0}^{\infty} \int_0^{\infty} dq \int_{-1}^1 dz \cdots \equiv \sum_{n=0}^{\infty} \Delta_n(k),\end{aligned}\tag{70}$$

where the dots indicate the integrand of the corresponding loop integrals (cf. appendix A 3), and we have put the external Matsubara frequency $k_0 = 0$ for convenience. In figure 2, we plot Δ_n multiplied by n^3 , as a function of the Matsubara summation index n . As can be clearly seen, the asymptotic behaviour $\Delta_n(k) \sim n^{-3}$ is reached very quickly at small momenta (left panel, $k = 0.5\mu$), for all temperatures down to $\beta = 20/\mu$. The same limit requires much more frequencies (up to 40) at large external momenta as demonstrated in the right panel ($k = 10\mu$). The asymptotics of the individual contribution allows for an accurate estimate of the remainder in the infinite Matsubara series. However, the $n = 0$ term still dominates in all cases,¹³ and the partial sum is found to always saturate once the asymptotic behaviour has set in. For instance, the worst convergence in figure 2 is at $k = 10\mu$ for the lowest temperature $\beta = 20/\mu$ (right panel). In this case, the asymptotics is not completely reached at $n = 20$, but the partial sum of the first 20 frequencies still agrees with the value extrapolated from the full asymptotic behaviour to better than 0.1%.

In figure 3, we show again $\Delta_n(k) n^3$, but this time on a linear plot which exhibits the slower convergence to the asymptotics more clearly. In the left panel of figure 3, we take a large momentum $k = 10\mu$ and study two different temperatures. It is apparent that $n = 30$ frequencies are enough to see the asymptotic behaviour and saturate the Matsubara sum at the intermediate temperature $\beta = 20/\mu$. As we further lower the temperature to $\beta = 100/\mu$, no sign of the correct asymptotics can be seen within the first 40 frequencies, although the $n = 0$ term still dominates in this case. The right panel of figure 3 shows that the convergence speed depends very much on the external momentum and, quite generally, decreases as the momentum is increased.

The bottom line is that summing up to $n = 30$ frequencies directly is sufficient to saturate the Matsubara sum for all relevant momenta down to temperatures of about $\beta = 20/\mu$, though as few as 4 frequencies are necessary at higher temperatures. By contrast, very low temperatures

¹³ This is not visible in the plot due to the factor n^3 .

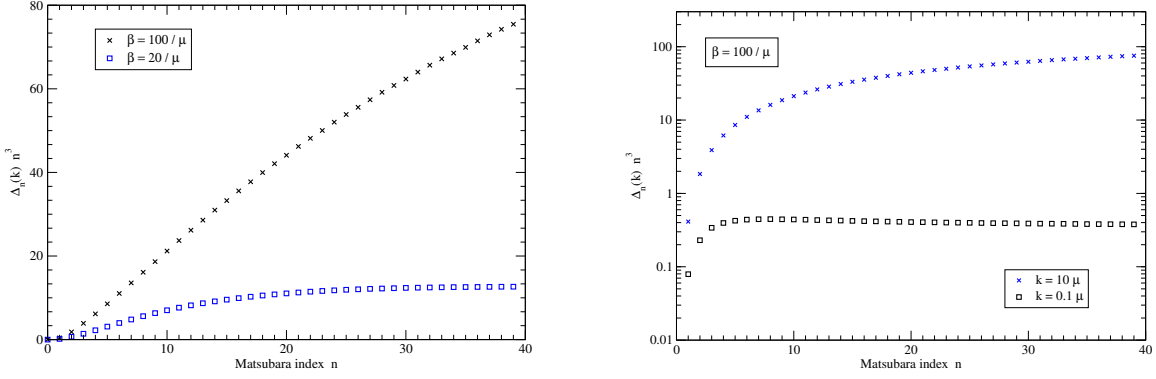


FIG. 3. The contribution $\Delta_n(k)$ of the n 'th Matsubara mode to the gluon form factor $\eta(0, k)$ at external momentum k . The left panel shows data for a large momentum $k = 10\mu$ and two different temperatures on a linear plot, while the right panel displays data for a very low temperature $\beta = 100/\mu$ at two different momenta k . Again, the contributions are multiplied by n^3 to better display their asymptotics.

can only be trusted for small momenta $k \ll \mu$, and would require an excessive amount of CPU time otherwise.¹⁴ We will mainly restrict our numerical effort to include up to $n = 20, \dots, 40$ frequencies at maximum, which means that we must content ourselves with temperatures not much below $\beta = 20/\mu$.

D. Comparision with lattice results

Finally, figure 4 and 5 show our cummulative results for the ghost and gluon propagator, respectively, at various temperatures compared to the $SU(3)$ lattice data taken from Ref. [13]. The lattice data was renormalized at a large scale $\mu_\infty = 5 \text{ GeV}$ in the perturbative region, with $\eta(0, \mu_\infty) = \mu_\infty^2 D_\perp(0, \mu_\infty) = \mu_\infty^2 D_\parallel(0, \mu_\infty) = 1$.

To translate this setting in our notation, we first set the arbitrary renormalization scale $\mu = \mu_\infty = 5 \text{ GeV}$, because μ is anyhow redundant once we change our renormalization prescription to match the lattice convention. In these units, the critical temperature is at $\beta^* = 16.67$. The lattice data goes down to temperatures of about $T = 0.67 T^*$, which translates into $\beta = 25$ which, according to the studies in the previous section, is still treatable with reasonable numerical effort. The gluon propagator normalization becomes $Z = \omega(0, \mu_\infty)/\mu^2 = 1/(D(0, \mu_\infty) \mu_\infty^2) = 1$. Finally, the intercept $\eta(0, \mu_c)$ is chosen at each temperature such that $\eta(0, \mu_\infty) = 1$ as discussed

¹⁴ Series accelerators also do not help in this case, since the eventual asymptotics has not been reached, cf. fig. 3.

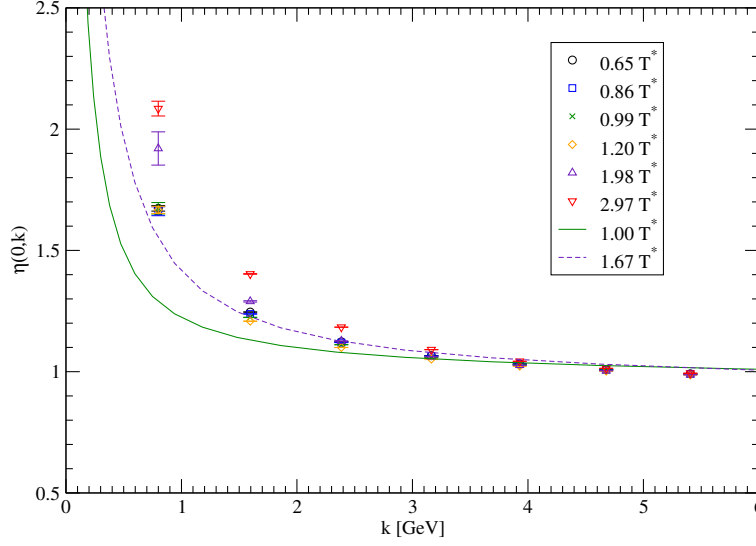


FIG. 4. The renormalized ghost form factor at various temperatures, as a function of the spatial momentum $k = |\mathbf{k}|$ with frequency $k_0 = 0$. Lattice data is taken from Ref. [13].

in the previous section. This fixes all the normalization, and leaves us with just the two fit parameters $m_{\perp}(\beta)/\mu$ and $m_{\parallel}(\beta)/\mu$ at each temperature.¹⁵

As can be seen from the plots, our approach is able to reproduce the basic properties of the propagators in full Yang-Mills theory at finite temperatures:

1. the gluon propagator is suppressed as the temperature increases
2. the ghost form factor is enhanced as the temperature increases
3. the temperature sensitivity of the *longitudinal* gluon propagator $D_{\parallel}(0, k)$ is much greater than for the transversal propagator (note the logarithmic scale in figure 5).

Quantitatively, the gluon propagator seems to miss some strength in the intermediate to low momentum regime, while the ghost form factor is too steep in this region. These problems seem, however, to be related to the determination of the overall scale $\mu = \mu_{\infty}$, which was taken from the match of the gluon propagator with the lattice data at $\mu = 5 \text{ GeV}$. As can be seen from figure 5, this determination is not very accurate as the propagators lie on top of each other for all temperatures at least down to about 3 GeV. Thus, there is some uncertainty of almost a factor of 2 in μ , which translates in the other dimensionfull quantities such as the

¹⁵ We set $\Delta m_{\parallel} = 0$ throughout as it has no effect on the final results.

norm of the gluon propagator or the mass parameters. Eventually, this scale should better be fixed intrinsically by computing a dimensionfull quantity such as the string tension from the Polyakov loop potential.

VI. SUMMARY AND CONCLUSIONS

In this paper, we have extended the covariant variational principle for Yang-Mills theory in Landau gauge to the case of non-zero temperatures. In the course of the derivation, we have also clarified and simplified the renormalization procedure at *zero* temperature, and re-determined the gluon mass parameter M_A (which is the only free parameter in our approach besides the overall normalization of the propagators) by comparison to lattice data. At finite temperatures, no further counter terms are necessary to put the system in a form that is manifestly independent of the UV cutoff, both in spatial and temporal momentum direction. We have carefully corroborated this cutoff-independence through numerical studies. Two mass parameters, which in principle are fixed from the $T = 0$ sector, had to be fitted to lattice data for practical reasons. The results are in qualitative agreement with recent high precision lattice data. We have also discussed possible causes of the discrepancy, which cannot be fixed reliably without an intrinsic determination of the scale μ .

The present framework allows for a number of further investigations. For instance, the question of possible deconfinement phase transition in our approach should be answered from the effective action for the Polyakov loop, which gives a much stronger argument than the $O(4)$ -symmetry violation in the propagators alone. This investigation is currently underway. In addition, the inclusion of fermions and a chemical potential is possible without further conceptional obstacles. To obtain realistic results, it may, however, be necessary to go beyond the Gaussian ansatz used in the present paper. This can be achieved e.g. with the Dyson-Schwinger method used in the context of variational calculations within the Hamiltonian approach in Coulomb gauge [43].

ACKNOWLEDGMENTS

The authors would like to thank A. Sternbeck for providing the lattice data used in section V. This work was supported by DFG under contract Re-856/9-1.

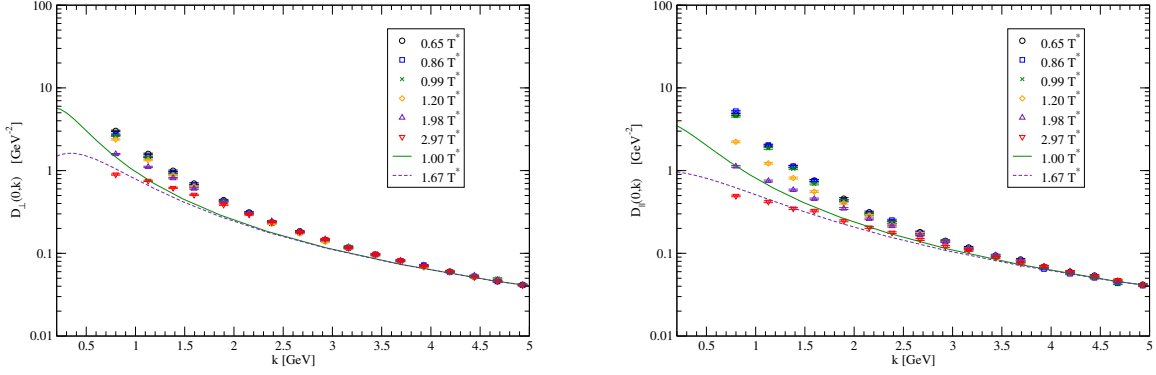


FIG. 5. The renormalized gluon propagator at various temperatures, as a function of the spatial momentum $k = |\mathbf{k}|$ with frequency $k_0 = 0$. The left panel shows the transversal component $D_{\perp}(0, k) = \bar{\omega}_{\perp}(0, k)^{-1}$, while the right panel shows the longitudinal component $D_{\parallel}(0, k) = \bar{\omega}_{\parallel}(0, k)^{-1}$. Lattice data is taken from Ref. [13].

Appendix A: Explicit calculations

1. The zero-temperature gap equation

In ref. [6] the (unrenormalized) gap equation at zero temperature was derived in the form

$$\begin{aligned} \bar{\omega}_0(k) &= k^2 + \chi_0(k) + M_0^2 & M_0^2 &= Ng^2 I_M^{(0)} \\ \chi_0(k) &= Ng^2 I_{\chi}^{(0)}(k) & \eta_0(k)^{-1} &= 1 - Ng^2 I_{\eta}^{(0)}(k), \end{aligned} \quad (\text{A1})$$

where the index '0' on all quantities indicates that these are the zero-temperature profiles. The integrals in this equation are given by

$$\begin{aligned} I_M^{(0)} &\equiv \frac{9}{4} \int \frac{d^4 q}{(2\pi)^4} \frac{1}{q^2 + M_0^2 + \chi_0(q)} \\ I_{\eta}^{(0)}(k) &\equiv \int \frac{d^4 q}{(2\pi)^4} \left[1 - (\hat{k} \cdot \hat{q})^2 \right] \frac{\eta_0(k - q)}{(k - q)^2 \bar{\omega}_0(q)} \\ I_{\chi}^{(0)}(k) &\equiv \frac{1}{3} \int \frac{d^4 q}{(2\pi)^4} \left[1 - (\hat{k} \cdot \hat{q})^2 \right] \frac{\eta_0(k - q) \eta_0(q)}{(k - q)^2}. \end{aligned} \quad (\text{A2})$$

2. Zero temperature mass functions

Here, we want to show the zero temperature limit

$$\lim_{\beta \rightarrow \infty} M_{\perp}^2(\beta) = M_0^2, \quad \lim_{\beta \rightarrow \infty} \Delta M_{\parallel}^2(\beta) = 0 \quad (\text{A3})$$

of the mass functions that appear in the gap equation (44) and (47) in the main text. We employ the auxiliary relation

$$\lim_{\beta \rightarrow \infty} \int_{\beta} \mathfrak{d}q f(q^2) \frac{\mathbf{q}^2}{q^2} = \frac{3}{4} \int \frac{d^4q}{(2\pi)^4} f(q^2), \quad (\text{A4})$$

which follows from $O(4)$ -invariance in the limit $\beta \rightarrow \infty$. If we use this relation and take the zero-temperature limit eq. (52) into account, we find

$$\begin{aligned} \lim_{\beta \rightarrow \infty} M_{\perp}^2(\beta) &= \frac{Ng^2}{2} \int \frac{d^4q}{(2\pi)^4} \frac{A+B(q)}{\bar{\omega}_0(q)} = \frac{Ng^2}{2} \int \frac{d^4q}{(2\pi)^4} \frac{\frac{14}{3} - \frac{2}{3} \frac{q_0^2}{q^2}}{\bar{\omega}_0(q)} \\ &= Ng^2 \int \frac{d^4q}{(2\pi)^4} \frac{1}{\bar{\omega}_0(q)} \left[2 + \frac{1}{3} \frac{\mathbf{q}^2}{q^2} \right] \\ &\stackrel{(\text{A3})}{=} Ng^2 \int \frac{d^4q}{(2\pi)^4} \frac{1}{\bar{\omega}_0(q)} \left[2 + \frac{1}{3} \cdot \frac{3}{4} \right] \\ &\stackrel{(\text{A2})}{=} M_0^2. \end{aligned}$$

The second equation (A3) follows in exactly the same manner.

3. Loop integrals at finite temperature

The integrals in the main result eq. (62) take the explicit form

$$\begin{aligned} I_{\eta}(k_0, |\mathbf{k}|) &= \int_{\beta} \mathfrak{d}q \frac{\eta(k-q)}{(k-q)^2} \frac{1 - (\hat{k} \cdot \hat{q})^2}{\bar{\omega}_{\parallel}(q)} \\ L_{\eta}(k_0, |\mathbf{k}|) &= \int_{\beta} \mathfrak{d}q \frac{\eta(k-q)}{(k-q)^2} (1 - (\hat{\mathbf{k}} \cdot \hat{\mathbf{q}})^2) \left[\bar{\omega}_{\perp}(q)^{-1} - \bar{\omega}_{\parallel}(q)^{-1} \right] \\ I_{\chi}^{\perp}(k_0, |\mathbf{k}|) &= \frac{1}{2} \int_{\beta} \mathfrak{d}q \frac{\eta(k-q) \eta(q)}{(k-q)^2} \frac{\mathbf{q}^2}{q^2} \left[1 - (\hat{\mathbf{k}} \cdot \hat{\mathbf{q}})^2 \right] \\ I_{\chi}^{\parallel}(k_0, |\mathbf{k}|) &= \int_{\beta} \mathfrak{d}q \frac{\eta(k-q) \eta(q)}{(k-q)^2} \left[\frac{q_0^2 + \mathbf{q}^2 (\hat{\mathbf{k}} \cdot \hat{\mathbf{q}})^2}{q^2} - (\hat{k} \cdot \hat{q})^2 \right] \\ M_{\perp}^2(\beta) &= \frac{1}{3} Ng^2 \int_{\beta} \mathfrak{d}q \left[\frac{4}{\bar{\omega}_{\perp}(q)} + \left(\frac{2q_0^2 + 3\mathbf{q}^2}{q_0^2 + \mathbf{q}^2} \right) \frac{1}{\bar{\omega}_{\parallel}(q)} \right] \\ \Delta M_{\parallel}^2(\beta) &= \frac{1}{3} Ng^2 \int_{\beta} \mathfrak{d}q \left[\frac{2}{\bar{\omega}_{\perp}(q)} + \left(\frac{q_0^2 - 3\mathbf{q}^2}{q_0^2 + \mathbf{q}^2} \right) \frac{1}{\bar{\omega}_{\parallel}(q)} \right]. \end{aligned} \quad (\text{A5})$$

For simplicity, we have written $\eta(q)$ etc. for the various form factors inside the loop integrals, although they depend, of course, on the two invariants q_0 and $|\mathbf{q}|$ separately.

4. Renormalization constants at finite temperature

As stated in the main text, the renormalized integral equation system eq. (64) contains five unknown, temperature-dependent constants which are all determined by zero-temperature counter terms. In detail, these relations are

$$\begin{aligned}
\eta(0, \mu_c)^{-1} &= \eta_0(\mu_c)^{-1} - \left[I_\eta(0, \mu_c) - I_\eta^{(0)}(\mu_c) - L_\eta(0, \mu_c) \right] &= \mu_0(\mu_c)^{-1} + \dots \\
\omega_\perp(0, \mu) &= Z \mu^2 + M_\perp^2(\beta) - M_0^2 + I_\chi^{(0)}(\mu) - I_\chi^\perp(0, \mu) &= Z \mu^2 + \dots \\
\omega_\parallel(0, \mu) &= Z \mu^2 + M_\perp^2(\beta) - M_0^2 + M_\parallel^2(\beta) + I_\chi^{(0)}(\mu) - I_\chi^\parallel(0, \mu) &= Z \mu^2 + \dots \\
\omega_\perp(0, \mu_0) &= Z M_A^2 + M_\perp^2(\beta) - M_0^2 + I_\chi^{(0)}(\mu_0) - I_\chi^\perp(0, \mu_0) &= Z M_A^2 + \dots \\
\omega_\parallel(0, \mu_0) &= Z M_A^2 + M_\perp^2(\beta) - M_0^2 + M_\parallel^2(\beta) + I_\chi^{(0)}(\mu_0) - I_\chi^\parallel(0, \mu_0) &= Z M_A^2 + \dots, \quad (\text{A6})
\end{aligned}$$

where the dots in the last form are the finite-temperature corrections to the zero-temperature renormalization data. These corrections are very hard to treat numerically because the corresponding difference of loop integrals involves the finite-temperature and zero-temperature form factors, respectively.

-
- [1] C. S. Fischer, J.Phys. **G32**, R253 (2006), arXiv:hep-ph/0605173 [hep-ph].
 - [2] R. Alkofer and L. von Smekal, Phys.Rept. **353**, 281 (2001), arXiv:hep-ph/0007355 [hep-ph].
 - [3] D. Binosi and J. Papavassiliou, Phys.Rept. **479**, 1 (2009), arXiv:0909.2536 [hep-ph].
 - [4] J. M. Pawłowski, Annals Phys. **322**, 2831 (2007), arXiv:hep-th/0512261 [hep-th].
 - [5] H. Gies, Lect.Notes Phys. **852**, 287 (2012), arXiv:hep-ph/0611146 [hep-ph].
 - [6] M. Quandt, H. Reinhardt, and J. Heffner, Phys.Rev. **D89**, 065037 (2014), arXiv:1310.5950 [hep-th].
 - [7] C. Feuchter and H. Reinhardt, Phys.Rev. **D70**, 105021 (2004), arXiv:hep-th/0408236 [hep-th].
 - [8] C. Feuchter and H. Reinhardt, (2004), arXiv:hep-th/0402106 [hep-th].
 - [9] I. Ojima, Nucl.Phys. **B143**, 340 (1978).
 - [10] T. Kugo and I. Ojima, Prog.Theor.Phys.Suppl. **66**, 1 (1979).
 - [11] A. Cucchieri and T. Mendes, PoS **LAT2007**, 297 (2007), arXiv:0710.0412 [hep-lat].
 - [12] A. Cucchieri and T. Mendes, Phys.Rev.Lett. **100**, 241601 (2008), arXiv:0712.3517 [hep-lat].
 - [13] I. Bogolubsky, E. Ilgenfritz, M. Muller-Preussker, and A. Sternbeck, Phys.Lett. **B676**, 69 (2009), arXiv:0901.0736 [hep-lat].
 - [14] A. Sternbeck and M. Muller-Preussker, PoS **ConfinementX**, 074 (2012), arXiv:1304.1416 [hep-lat].

- [15] C. S. Fischer, A. Maas, and J. M. Pawłowski, *Annals Phys.* **324**, 2408 (2009), arXiv:0810.1987 [hep-ph].
- [16] A. Aguilar and A. Natale, *JHEP* **0408**, 057 (2004), arXiv:hep-ph/0408254 [hep-ph].
- [17] A. Aguilar and J. Papavassiliou, *Phys.Rev.* **D77**, 125022 (2008), arXiv:0712.0780 [hep-ph].
- [18] A. C. Aguilar and J. Papavassiliou, *Eur.Phys.J.* **A35**, 189 (2008), arXiv:0708.4320 [hep-ph].
- [19] D. Binosi and J. Papavassiliou, *Phys.Rev.* **D77**, 061702 (2008), arXiv:0712.2707 [hep-ph].
- [20] A. Aguilar, D. Binosi, and J. Papavassiliou, *Phys.Rev.* **D78**, 025010 (2008), arXiv:0802.1870 [hep-ph].
- [21] P. Boucaud, T. Bruntjen, J. Leroy, A. Le Yaouanc, A. Lokhov, *et al.*, *JHEP* **0606**, 001 (2006), arXiv:hep-ph/0604056 [hep-ph].
- [22] P. Boucaud, J.-P. Leroy, A. L. Yaouanc, J. Micheli, O. Pene, *et al.*, *JHEP* **0806**, 012 (2008), arXiv:0801.2721 [hep-ph].
- [23] P. Boucaud, J. Leroy, A. Le Yaouanc, J. Micheli, O. Pene, *et al.*, *JHEP* **0806**, 099 (2008), arXiv:0803.2161 [hep-ph].
- [24] D. Dudal, R. Sobreiro, S. Sorella, and H. Verschelde, *Phys.Rev.* **D72**, 014016 (2005), arXiv:hep-th/0502183 [hep-th].
- [25] D. Dudal, S. Sorella, N. Vandersickel, and H. Verschelde, *Phys.Rev.* **D77**, 071501 (2008), arXiv:0711.4496 [hep-th].
- [26] M. Capri, D. Dudal, V. Lemes, R. Sobreiro, S. Sorella, *et al.*, *Eur.Phys.J.* **C52**, 459 (2007), arXiv:0705.3591 [hep-th].
- [27] D. Dudal, J. A. Gracey, S. P. Sorella, N. Vandersickel, and H. Verschelde, *Phys.Rev.* **D78**, 065047 (2008), arXiv:0806.4348 [hep-th].
- [28] O. Oliveira and P. Silva, *Eur.Phys.J.* **C62**, 525 (2009), arXiv:0705.0964 [hep-lat].
- [29] O. Oliveira and P. Silva, *Phys.Rev.* **D79**, 031501 (2009), arXiv:0809.0258 [hep-lat].
- [30] J. Rodriguez-Quintero, *JHEP* **1101**, 105 (2011), arXiv:1005.4598 [hep-ph].
- [31] M. Q. Huber and L. von Smekal, *JHEP* **1304**, 149 (2013), arXiv:1211.6092 [hep-th].
- [32] M. Pelàez, M. Tissier, and N. Wschebor, *Phys.Rev.* **D90**, 065031 (2014), arXiv:1407.2005 [hep-th].
- [33] D. Schutte, *Phys.Rev.* **D31**, 810 (1985).
- [34] A. P. Szczepaniak and E. S. Swanson, *Phys.Rev.* **D65**, 025012 (2002), arXiv:hep-ph/0107078 [hep-ph].
- [35] H. Reinhardt and C. Feuchter, *Phys.Rev.* **D71**, 105002 (2005), arXiv:hep-th/0408237 [hep-th].
- [36] D. Epple, H. Reinhardt, and W. Schleifenbaum, *Phys.Rev.* **D75**, 045011 (2007), arXiv:hep-th/0612241 [hep-th].
- [37] J. M. Pawłowski, *Nucl.Phys.* **A931**, 113 (2014).
- [38] C. A. Welzbacher, C. S. Fischer, and J. Luecker, (2014), arXiv:1412.3650 [hep-ph].

- [39] U. Reinosa, J. Serreau, M. Tissier, and N. Wschebor, Phys.Lett. **B742**, 61 (2015), arXiv:1407.6469 [hep-ph].
- [40] U. Reinosa, J. Serreau, M. Tissier, and N. Wschebor, Phys.Rev. **D91**, 045035 (2015), arXiv:1412.5672 [hep-th].
- [41] R. Aouane, V. Bornyakov, E. Ilgenfritz, V. Mitrjushkin, M. Muller-Preussker, *et al.*, Phys.Rev. **D85**, 034501 (2012), arXiv:1108.1735 [hep-lat].
- [42] C. W. Bernard, Phys.Rev. **D9**, 3312 (1974).
- [43] D. R. Campagnari and H. Reinhardt, Phys.Rev. **D82**, 105021 (2010), arXiv:1009.4599 [hep-th].